NATIONAL ADVISORY COMMITTEE FOR AERONAUTICS

TECHNICAL NOTE

No. 1252

INTERFERENCE METHOD FOR OBTAINING THE POTENTIAL FLOW PAST AN ARBITRARY CASCADE OF AIRFOILS

By S. Katzoff, Robert S. Finn, and James C. Laurence

Langley Memorial Aeronautical Laboratory
Langley Field, Va.

Washington
May 1947

NATIONAL ADVISORY COMMITTEE FOR AERONAUTICS

TECHNICAL NOTE NO. 1252

INTERFERENCE METHOD FOR OBTAINING THE POTENTIAL FLOW PAST AN ARBITRARY CASCADE OF AIRFOILS

By S. Katzoff, Robert S. Finn, and James C. Laurence

SUMMARY

A procedure is presented for obtaining the pressure distribution in a two-dimensional, incompressible, and nonviscous flow on an arbitrary airfoil section in cascade. The method considers directly the influence on a given airfoil of the rest of the cascade and evaluates this interference by an iterative process, which appeared to converge rapidly in the cases tried (about unit solidity, stagger angles of 0° and 45°). Two variations of the basic interference calculations are described. One, which is accurate enough for most purposes, involves the substitution of sources, sinks, and vortices for the interfering airfoils; the other, which may be desirable for the final approximation, involves a contour integration. The computations are simplified by the use of a chart presented by Betz in a related paper. The numerical labor involved, while considerable, is less than that required by the present methods of conformal transformation. Illustrative examples are included.

INTRODUCTION

The rapid increase of interest in the design of fans and turbines has led to many studies of the two-dimensional flow past infinite lattices. Most of these studies involve approximate procedures (for example, references 1 to 3) or present solutions for special classes of shapes (references 4 and 5). Recently, attempts have been made to obtain exact solutions by conformal transformation of the lattice to a circle. To this end, Howell (reference 6) used a procedure that first transformed the lattice to an isolated S-shape figure, which could then be transformed to a near circle by successive Joukowski transformations and finally to a circle by the method of reference 7. In reference 8 the cascade was transformed first to a near circle and then to a circle, also with the use of several stages of conformal mapping. In reference 9 the lattice was mapped into a lattice of straight

parallel lines by means of a function that was determined with the aid of the transformation of this line lattice to a circle. (See references 10 and 11.) These transformations are of considerable interest, theoretically. The methods of references 6 and 8 require lengthy computations, however, and difficulty has been experienced in obtaining accurate numerical results with the method of reference 9. All three methods require modifications for highly cambered contours or for lattices of high stagger and solidity.

The method presented herein does not seek a conformal transformation directly but, like the older approximate methods, seeks to evaluate the interference at each airfoil due to the presence of all the other airfoils of the cascade. The velocity distribution on each airfoil is considered to be the sum of that corresponding to its presence in the uniform free-stream flow plus that corresponding to its presence in the interference flow. The interference is calculated from the velocity distribution on the airfoils so that the method reduces to an iteration process in which, for the first approximation, the interference is computed by assuming the free-stream velocity distribution to exist on each airfoil, and in subsequent approximations this velocity is corrected according to the interference derived in the preceding approximation. A solution is thus found for an arbitrarily specified angle of attack, and this solution is used to find the conformal transformation to the circle and thence the solution for any other angle of attack.

The present method has been found appreciably less laborious than the methods that seek the conformal transformation directly and is also considered more flexible in that it may be adapted to a variety of cascade problems that would be difficult to solve by formal transformation methods; for example, the problem of the flow about double cascades (or superimposed lattices) or certain types of "inverse" problems involving the determination of the setting or solidity for a given airfoil in cascade. Some of the features of the interference and iteration methods used should also be useful in the solution of flows involving a finite number of interfering bodies.

SYMBOLS

W	flow function (complex potential)
Φ	velocity potential
Ψ	stream function

V	velocity at infinity
Γ	circulation
K	mapping-function parameter
v	local velocity
γ	vortex strength
m	source strength
z	complex variable of physical plane $(x + iy)$
z'	fixed point in physical plane
ζ	complex variable of reference plane $(\xi + i\eta)$
c	profile chord
c_1	profile chord used in transformation of reference 7
d	cascade spacing (distance between corresponding points on adjacent blades; see fig. 1)
φ	central angle of perfect circle obtained in transformation of reference 7
θ	central angle of unit circle of figure 1
s	surface length on profile
β	blade angle (angle between stagger line and normal to chords; see fig. 1)
σ	solidity (ratio of chord to distance between profiles)
λ	angle between flow direction and normal to stagger line
α	angle of attack relative to blade chord
η	angle of zero lift for cascade, relative to blade chord
Δp	static pressure rise
ω	turning angle of flow

ρ density of fluid

a_n, b_n Fourier series coefficients

Subscripts:

f free stream

d disturbance

c compensating

Γ due to circulation change

a additional

T total

t tail stagnation point

n nose stagnation point

T.E. trailing edge

s due to source rows

v due to vortex rows

z physical plane

ζ reference plane

0 mean flow

1 incoming flow

2 outgoing flow

λ_0 at flow direction λ_0

λ_0' at flow direction λ_0'

THEORY OF INTERFERENCE CALCULATIONS

In order to explain better the basic concepts and procedures of the interference calculations, discussion of the iteration steps will

be postponed for the present, and the interference calculations will be described as if they were being used to verify a known solution.

Breakdown of the flow function into four components.- Attention is fixed on one airfoil of the infinite cascade which will be designated the central airfoil. The flow function on the boundary of this airfoil is considered to be the sum of the following components:

W_f the flow function for the central airfoil, considered as isolated in the free-stream flow (the vector average of the flow far in front of the cascade and the flow far behind the cascade). Inasmuch as the boundary is a streamline in this flow, $W_f = \Phi_f$.

W_d the disturbance along the contour caused by the presence of all the other airfoils of the cascade, designated the external airfoils $\left(W_d = \Phi_d + i\Psi_d\right)$

W_c the compensating flow function (which may have singularities only within the central airfoil) that is required to maintain the airfoil a streamline in the presence of the disturbance flow. It is determined by the condition that, on the boundary, its stream function must be equal and opposite to the disturbance stream function. Thus, $W_c = \Phi_c + i\Psi_c$, where $\Psi_c = -\Psi_d$.

W_Γ the contribution of the circulation that must be added to maintain the trailing-edge condition; it has only a real component $\left(W_\Gamma = \Phi_\Gamma\right)$

The sum $W_d + W_c + W_\Gamma$ represents the net change of flow function due to the presence of the external airfoils; it will be designated the additional flow function $W_a = \Phi_a$. The sum $W_a + W_f$ will be designated the total flow function $W_T = \Phi_T$.

The evaluation of the isolated, or free-stream, flow Φ_f is readily performed by the method of reference 7 and requires no further discussion in the present paper. The disturbance flow can be calculated when the potential distribution (or velocity distribution) on the external airfoils is known. Finally, the compensating flow and the circulation flow are readily determined, as will be shown, when the disturbance flow is known. In the following sections two methods of calculating the disturbance flow will be described: the approximate source-vortex method and the exact contour-integral method.

Disturbance flow by approximate source-vortex method.- Each of the external airfoils is considered to be adequately represented by an arrangement of about two sources, three sinks (or negative sources), and five vortices distributed along its mean line. The strengths and locations of these singularities are chosen on the basis of the chordwise thickness distribution and chordwise velocity distribution. The choice is somewhat arbitrary and may be left to the judgement of the worker; however, a detailed method of choice has been described in the section entitled "Computational Methods." The disturbance flow, then, is that of about ten infinite rows of singularities, equally spaced along the cascade direction except that none are located where the central airfoil is to be placed. The field of each vortex row is shown in figure 2 where, for convenience, the vortices are assumed to be of unit strength, spaced at unit distance along the y-axis. This figure is from reference 1 and the equation for the flow is (reference 2)

$$W = -\frac{i}{2\pi} \log_e \sinh \pi z + \frac{i}{2\pi} \log_e \pi z$$

In order to find the contribution to the disturbance flow caused by a row of vortices at, say, 0.3 chord on the external airfoils, the central airfoil, drawn to scale and properly oriented relative to the cascade direction, is placed at the center of figure 2, with the origin at 0.3 chord on the mean line. The values of velocity potential and stream function read at selected points along the airfoil contour, multiplied by the assumed vortex strength, give directly the contribution of this vortex row to Φ_d and Ψ_d. By shifting the central airfoil so that the origin is located, in turn, at each of the other assumed vortex positions along the mean line and repeating the foregoing process, the contributions of all the vortices in the external airfoils are obtained at the same points. The sum of these values at a given point on the central airfoil represents the contribution of the vortex singularities in the lattice to the disturbance function W_d at that point. The contributions of the sources can be found in the same way except that the lines marked Ψ are considered as $-\Phi$ and the lines marked Φ are considered as Ψ. Sinks are considered as negative sources.

Contour-integral method for evaluating disturbance flow function.- In the preceding section, the disturbance field was calculated approximately by representing each airfoil by a somewhat arbitrary arrangement of vortices, sources, and sinks distributed on the mean line. An airfoil may be represented exactly by a continuous distribution of vortices along its contour, the linear density of which at every point equals the velocity on the airfoil

at that point (reference 12). The field at a point on the central airfoil due to a row of corresponding surface elements of the external airfoils (that is, a row of vortices of strength $v_T\,ds$) may be obtained directly from figure 2. Integration of this contribution along the contours of the external airfoils provides an exact determination of the disturbance field. The procedure is an obvious modification of the preceding approximate method.

Let Φ and Ψ (without subscripts) denote, respectively, the potential and stream function of the row of unit vortices in figure 2. In order to determine the disturbance potential and stream function at a point z' on the central airfoil, the airfoil contour, drawn to scale and correctly oriented relative to the cascade direction, is superimposed on figure 2 so that the origin falls, in turn, at a number of points z on the contour, and for each setting values of Φ and Ψ are read at the point z'. Then the disturbance flow function at z' is given by

$$\Phi_d(z') = \int_c \Phi\, v_T(z)\, ds$$

$$\Psi_d(z') = \int_c \Psi\, v_T(z)\, ds$$

where

$v_T(z)$ local velocity on the airfoil at variable point z

s distance along airfoil contour

Φ, Ψ values read at z' when origin of figure 2 is at z

and the integration is performed along the airfoil contour. Since $v_T(z)\,ds = d\Phi_T(z)$, the foregoing equations can be rewritten as

$$\Phi_d(z') = \int_c \Phi\, d\Phi_T(z)$$

$$\Psi_d(z') = \int_c \Psi\, d\Phi_T(z)$$

so that the disturbance potential and stream function at point z' are readily evaluated by plotting Φ and Ψ against Φ_T and measuring the area under the curves.

Determination of compensating flow and circulation flow.- As has been indicated, the compensating flow function may have singularities only within the central airfoil contour, and on the contour, the stream function must be exactly equal and opposite to the disturbance stream function. From the known transformation of the isolated airfoil to the circle, which was found in the process of determining W_f, the correspondence between points on the airfoil and points on the circle is known. If, then, the desired compensating stream function is expanded as a Fourier series in terms of the circle angle φ,

$$\Psi_c = \sum_{n=1}^{\infty} (a_n \cos n\varphi + b_n \sin n\varphi)$$

its corresponding velocity potential will be (reference 7) the conjugate series

$$\Phi_c = \sum_{n=1}^{\infty} (-b_n \cos n\varphi + a_n \sin n\varphi)$$

The determination of Φ_c from Ψ_c is readily accomplished by the method of reference 13.

In order to maintain the trailing-edge condition, a vortex Γ_a must be added at the center of the circle of such strength that $\Gamma_a/2\pi$ equals the value of $-d\Phi_c/d\varphi$ at the trailing edge (determined graphically from a faired plot of Φ_c against φ). The corresponding contribution to the potential is

$$\Phi_\Gamma = \frac{\Gamma_a}{2\pi}\varphi$$

The velocity potential $\Phi_a = \Phi_d + \Phi_c + \Phi_\Gamma$ that constitutes the net effect of putting the airfoil in the cascade (that is, the net interference effect) may now be determined by simple addition of the three components. Presumably, since the calculations were made with the correct Φ_T, Φ_a should be the difference between Φ_f and Φ_T.

In the final step, Φ_a is differentiated with respect to distance along the airfoil to get the corresponding interference effect on the velocity v_a which should be the difference between v_f and v_T. Convenient procedures for performing these calculations are discussed in the section entitled "Computational Methods."

ITERATION METHOD

In the preceding sections the basic concepts and procedures of cascade interference calculations have been outlined. In the present section, the application of such calculations in the proposed iteration method of solving cascade flow will be discussed.

As first attempted, the method was essentially as follows: In the first step, Φ_T is assumed to equal Φ_f and a first approximation to Φ_a is calculated on this basis by the methods just described. In the second step, Φ_T is assumed equal to the sum of Φ_f and this first approximation to Φ_a, and a second approximation to Φ_a is computed. The succeeding steps follow the same pattern and are continued until two successive Φ_a-distributions are essentially the same. The source-vortex method was used for the earlier approximations, but the final approximation, when convergence is practically complete, was made by the contour-integral method. This procedure, however, was found to converge relatively slowly in some cases; and the general practicability of the interference method depends on a slight modification of the source-vortex method.

The modification depends upon the observations that the contribution of the sources and sinks to Φ_a changes by relatively little from one approximation to the next and that the contribution of the vortices to Φ_a is nearly proportional to their total strength and relatively independent of their distribution. Obviously, if it were exactly true that the contribution of the sources and sinks is constant and that the contribution of the vortices is proportional to their total strength, only one interference calculation would be required and the solution could then be obtained through a simple algebraic equation. Thus, let

Γ_T total circulation on airfoil in cascade

Γ_f total circulation on isolated airfoil at same angle of attack

Γ_a additional circulation $\left(\Gamma_T - \Gamma_f\right)$

Γ_{a_s} constant contribution of sources and sinks to Γ_a

Γ_{a_v} contribution of vortices to Γ_a when Γ_f is assumed on all external airfoils

Then, by the preceding assumptions,

$$\Gamma_T = \Gamma_f + \Gamma_{a_s} + \frac{\Gamma_T}{\Gamma_f}\Gamma_{a_v}$$

whence

$$\Gamma_T = \frac{\Gamma_f + \Gamma_{a_s}}{1 - \frac{\Gamma_{a_v}}{\Gamma_f}} \qquad (1)$$

Since the assumptions are not exactly true, the value of Γ_T so calculated is correspondingly inexact; however, it is much closer to the true value than if it were taken simply as $\Gamma_f + \Gamma_{a_s} + \Gamma_{a_v}$. Correspondingly, the potential $\Phi_T = \Phi_f + \Phi_{a_s} + \frac{\Gamma_T}{\Gamma_f}\Phi_{a_v}$ is much more accurate than the sum $\Phi_f + \Phi_{a_s} + \Phi_{a_v}$.

The second approximation is similarly adjusted. Thus, corresponding to the Φ_T-distribution just obtained, a new set of sources, sinks, and vortices are distributed along the mean line, and new values of Γ_{a_s} and Γ_{a_v} are calculated. Adjustment follows, as before, from the equation

$$\Gamma_{T_2} = \Gamma_f + \Gamma_{a_s} + \frac{\Gamma_{T_2}}{\Gamma_{T_1}}\Gamma_{a_v}$$

where the subscripts 1 and 2 refer to the first and second approximations, respectively. Solution for Γ_{T_2} gives

$$\Gamma_{T_2} = \frac{\Gamma_f + \Gamma_{a_s}}{1 - \frac{\Gamma_{a_v}}{\Gamma_{T_1}}} \qquad (2)$$

and, finally, the potential is given by

$$\Phi_{T_2} = \Phi_f + \Phi_{a_s} + \frac{\Gamma_{T_2}}{\Gamma_{T_1}} \Phi_{a_v}$$

This simple modification of the procedure is so effective that in the cases tried, the first step gave solutions that would be satisfactory for many purposes and the procedure had practically converged at the second step. The additional complication of keeping the source-sink and the vortex effects separate so that Γ_{a_s} and Γ_{a_v} can be separately computed is relatively minor and amply repaid by the rapidity of convergence.

After the source-vortex method has essentially converged, a final approximation by the contour-integral method is desirable. In the cases computed, however, this final step was found to introduce only minor changes in the result.

THE FLOW AT OTHER ANGLES OF ATTACK

From a known velocity distribution at a given angle of attack, the angle of zero lift and the slope of the lift curve, together with the velocity distribution at any other angle of attack, may be obtained. For this purpose, the lattice is conveniently considered to be related conformally to an isolated circle by a periodic transformation, which might be, say, of the type used in reference 6, 8, or 9. The explicit form of the transformation, however, is not needed for the present purpose.

The flow function in the circle (ζ) plane that corresponds to the desired flow in the physical (z) plane is

$$W = -\frac{V_0 d}{2\pi}\left(e^{-i\lambda_0} \log_e \frac{\zeta + e^K}{\zeta - e^K} + e^{i\lambda_0} \log_e \frac{\zeta + e^{-K}}{\zeta - e^{-K}}\right) - \frac{i\Gamma}{4\pi} \log_e \frac{\zeta^2 - e^{2K}}{\zeta^2 - e^{-2K}} \qquad (3)$$

In the ζ-plane this flow may be interpreted as that due to the system of sources, sinks, and vortices shown in figure 1. The unit circle $\zeta = e^{i\theta}$ is a streamline of the flow and the circulation about any contour enclosing this circle but not enclosing the points $\zeta = \pm e^{k}$ is Γ (positive clockwise).

In the physical (z) plane, the complex velocities at the points $z = \infty$ and $z = -\infty$ are determined by equation (3) and the transformation. Thus,

$$\left(\frac{dW}{dz}\right)_{\infty} = -V_0 e^{-i\alpha_0} + i\frac{\Gamma}{2d}e^{i\beta} = -V_1 e^{-i\alpha_1}$$

and

$$\left(\frac{dW}{dz}\right)_{-\infty} = -V_0 e^{-i\alpha_0} - i\frac{\Gamma}{2d}e^{i\beta} = -V_2 e^{-i\alpha_2}$$

where the angles and velocities are defined in figure 1. The flow far from the lattice is seen to be the same as that of an infinite vortex row in the uniform flow $-V_0 e^{-i\alpha_0}$. It should be noted (fig. 1) that $\lambda_0 = \alpha_0 + \beta$, $\lambda_1 = \alpha_1 + \beta$, and $\lambda_2 = \alpha_2 + \beta$. In the following paragraphs it will be shown how to obtain from the given solution in cascade the parameter K and the stagnation points θ_n and θ_t for the corresponding flow about the circle. These values fix the angle of zero lift and the slope of the lift curve of the airfoil in cascade; together with the known potential distribution they determine the conformal correspondence between the profile and the circle and, hence, the velocity distribution at any angle of attack.

Since the airfoil contour (z-plane) is conformally related to the unit circle (ζ-plane), it follows that at any given angle of attack α_0, the change of velocity potential from nose to tail stagnation point on both upper and lower surfaces must be the same for the circle and for the profile in cascade. These potential changes can readily be obtained for the single solution on the lattice from the final Φ_T-distribution. The velocity potential on the unit circle is obtained from equation (3). Thus,

$$\frac{\Phi_\zeta}{cV_0} = -\frac{1}{2\pi\sigma}\left[\cos\lambda_0 \log_e\left(\frac{\cosh K + \cos\theta}{\cosh K - \cos\theta}\right) + 2\sin\lambda_0 \tan^{-1}\frac{\sin\theta}{\sinh K} + \frac{\Gamma}{V_0 d}\tan^{-1}\frac{\tan\theta}{\tanh K}\right] \tag{4}$$

and the change of potential from nose stagnation point θ_n to tail stagnation point θ_t is

$$\frac{\Delta\Phi_\zeta}{cV_0} = \frac{1}{2\pi\sigma}\left\{\cos\lambda_0 \log_e\left[\frac{(\cosh K - \cos\theta_t)(\cosh K + \cos\theta_n)}{(\cosh K + \cos\theta_t)(\cosh K - \cos\theta_n)}\right] + 2\sin\lambda_0 \tan^{-1}\left[\frac{(\sin\theta_n - \sin\theta_t)\sinh K}{\sinh^2 K + \sin\theta_n \sin\theta_t}\right] + \frac{\Gamma}{V_0 d}\tan^{-1}\left[\frac{(\tan\theta_n - \tan\theta_t)\tanh K}{\tanh^2 K + \tan\theta_n \tan\theta_t}\right]\right\} \tag{5}$$

This potential change may be obtained for either the upper or the lower surface. Two values are obtained depending on the choice of quadrant for the third term of equation (5). The condition of zero velocity at nose and tail stagnation points is

$$\sin\theta\cos\lambda_0 - \cos\theta\tanh K\sin\lambda_0 - \frac{\Gamma}{2V_0 d}\sinh K = 0 \tag{6}$$

By use of the known values of Γ, $\Delta\Phi_T$, and λ_0, equations (5) and (6) can be solved simultaneously for θ_n, θ_t, and K. Equation (6) can be considered as a quadratic in $\sin\theta$ and with an assumed value of K determines corresponding values of θ_n and θ_t. Equation (5) then determines $\Delta\Phi_\zeta$. By the proper choice of values of K, a curve of $\Delta\Phi_\zeta$ against K may be plotted such that at a point on this curve $\Delta\Phi_\zeta = \Delta\Phi_T$. The value of K at this point is the desired value; the corresponding values of θ_n and θ_t

are then given by equation (6). A convenient initial choice for K is the value that corresponds to a lattice of straight lines of the same stagger and of about 10 percent or 20 percent higher solidity. Figure 3 is of aid in this respect. The computed values of K and θ_t, together with equation (6), determine the angle of zero lift [$\Gamma = 0$] with respect to the airfoil chord, thus,

$$\eta = \tan^{-1} \frac{\tan \theta_t}{\tanh K} - \beta \qquad (7)$$

and the slope of the lift curve, based on mean velocity, is obtained by differentiating equation (6) with respect to λ_0; thus,

$$\frac{dc_l}{d\alpha_0} = \frac{4}{\sigma} \frac{\sqrt{\sin^2\theta_t + \sinh^2 K}}{\sinh K \cosh K} \qquad (8)$$

A correspondence between points on the airfoil and points on the unit circle may be obtained by comparing the values of Φ_ζ computed by equation (4) with the values of Φ_T from the known potential distribution. The points (x,y) on the profile and θ on the circle for which $\Phi_\zeta = \Phi_T$ are corresponding points. The velocity on the lattice profile for the stream angle λ_0 is

$$\left(\frac{v}{V_0}\right)_{\lambda_0} = \left|\frac{d\zeta}{dz}\right| \frac{1}{V_0} \frac{d\Phi_\zeta}{d\theta}$$

$$= \left|\frac{d\zeta}{dz}\right| \frac{d}{\pi} \left[\frac{\cos \lambda_0 \cosh K (\sin \theta - \sin \theta_t) - \sin \lambda_0 \sinh K (\cos \theta - \cos \theta_t)}{\cosh^2 K - \cos^2 \theta} \right]$$

where the term in brackets, which represents the velocity on the circle boundary, is obtained by differentiating equation (4). It follows that the velocity corresponding to a new stream angle λ_0' is

$$\left(\frac{v}{V_0}\right)_{\lambda_0'} = \left(\frac{v}{V_0}\right)_{\lambda_0} \left[\frac{\cos\lambda_0' \cosh K(\sin\theta - \sin\theta_t) - \sin\lambda_0' \sinh K(\cos\theta - \cos\theta_t)}{\cos\lambda_0 \cosh K(\sin\theta - \sin\theta_t) - \sin\lambda_0 \sinh K(\cos\theta - \cos\theta_t)}\right] \quad (9)$$

The following relations, which describe the flow far away from the lattice, are of interest. The stream angles λ_1 and λ_2 at $z = \infty$ and $z = -\infty$ are

$$\lambda_1 = \tan^{-1} \frac{\sin\lambda_0 + \frac{\Gamma}{2V_0 d}}{\cos\lambda_0}$$

and

$$\lambda_2 = \tan^{-1} \frac{\sin\lambda_0 - \frac{\Gamma}{2V_0 d}}{\cos\lambda_0}$$

and the angle through which the fluid is turned by the lattice is given by

$$\omega = \tan^{-1} \frac{\frac{\Gamma}{V_0 d}\cos\lambda_0}{1 - \left(\frac{\Gamma}{2V_0 d}\right)^2}$$

The rise in static pressure across the lattice is

$$\frac{\Delta p}{\frac{1}{2}\rho V_0^2} = \left(\frac{V_1}{V_0}\right)^2 - \left(\frac{V_2}{V_0}\right)^2$$

$$= \cos^2\lambda_0 \left(\sec^2\lambda_1 - \sec^2\lambda_2\right)$$

REMARKS ON CONTOUR MODIFICATIONS CORRESPONDING TO LOCAL PRESSURE CHANGES

In reference 14, the modification of an airfoil contour to obtain, approximately, desired small changes in the pressure distribution is discussed. The method, based on the formulas of reference 7, evaluates a slight modification of the conformal transformation of the circle to the airfoil, such that the stretching factor at every point is changed in proportion to the desired relative change in local velocity.

Although in reference 14 the airfoil was assumed to lie in a straight uniform field, the treatment is equally applicable when the airfoil is in a curved or distorted flow field. Accordingly, the procedure should be applicable to airfoils in cascade, provided the same modification of the external airfoils leaves the disturbance flow field essentially unaffected. This condition may not always be satisfied; however, in such cases the method could possibly be improved by a procedure analogous to that described in the section of the present paper entitled "Iteration Method."

COMPUTATIONAL METHODS

The basic theory has been presented. In the following sections some of the methods used for performing the actual computations will be discussed.

Selection of points for evaluation of disturbance flow.- The determination of the compensating flow by the method of reference 13 requires that the disturbance flow be evaluated at points that, by the conformal transformation, correspond to points equally spaced about the circle. These points, which are located by reference to the conformal transformation, are preferably chosen so that one is at the trailing edge. Experience has shown that, for the preliminary approximations, 12 points at 30° intervals yield acceptable results. In the final step by the contour-integral method, the use of 24 points is preferable in order to improve accuracy, especially near the nose. An acceptable compromise is to evaluate Φ_d and Ψ_d directly for only the additional points that are near the leading edge and to pick off the values at the other additional points from a faired curve.

Inasmuch as values for the 12-point and 24-point methods are not included in reference 13 the following table is presented:

k	C_k	
	n = 6	n = 12
1	0.62201	0.63298
3	.16667	.20118
5	.04466	.10860
7	------	.06394
9	------	.03452
11	------	.01097

Evaluation of Φ_f and v_a.- Integration of equation (36) of reference 7 along the circle boundary yields the values of the potential Φ_f at points on the airfoil as follows:

$$\frac{\Phi_f}{V_0} = 2ae^{\Psi_0}\left[\varphi \sin(\alpha + \beta) - \cos(\alpha + \varphi)\right] \qquad (10)$$

where

α angle of attack

β angle of attack for zero lift

ae^{Ψ_0} radius of the circle to which the airfoil transforms

φ angular position along the circle, as determined by the transformation

If the transformation has been performed as recommended in reference 7, the constant (a) will be slightly less than one fourth the chord. Although the potential discontinuity (corresponding to the circulation) may, without loss of generality, be placed at any point on the contour, the trailing edge will generally be found to be the most convenient location.

The additional velocity v_a is given by the derivative along the surface $\frac{d\Phi_a}{ds}$; it may be determined by graphically differentiating Φ_a with respect to the circle angle φ and multiplying this slope by $\frac{d\varphi}{ds}$. Thus,

$$\frac{v_a}{V_0} = \frac{d\Phi_a}{V_0 ds} = \frac{d\Phi_a}{V_0 d\varphi}\frac{d\varphi}{ds} \tag{11}$$

The value of $\frac{d\varphi}{ds}$ may be obtained from equations (37) and (38) of reference 7. Thus,

$$\left|\frac{dz}{d\zeta}\right| = ae^{\Psi_0}\frac{d\varphi}{ds} = \frac{\left(1 + \frac{d\epsilon}{d\theta}\right)e^{\Psi_0}}{2\sqrt{\left[1 + \left(\frac{d\Psi}{d\theta}\right)^2\right]\left[\sinh^2\Psi + \sin^2\theta\right]}} \tag{12}$$

or

$$\frac{d\varphi}{ds} = \frac{1 + \frac{d\epsilon}{d\theta}}{2a\sqrt{\left[1 + \left(\frac{d\Psi}{d\theta}\right)^2\right]\left[\sinh^2\Psi + \sin^2\theta\right]}}$$

where the symbols ϵ, θ, and Ψ are defined in reference 7.

The cascade solidity need be taken into account only when the airfoil sketch to be used with figure 2 is constructed. For the subsequent calculations, any convenient airfoil chord may be used, provided only that the same chord is used for the external airfoils and for the central airfoil. The reason is as follows: The strengths of the singularities used to represent the external airfoils are proportional to the assumed airfoil chord; hence the additional potentials induced on the central airfoil will be proportional to the assumed chord. Since both the additional

potential Φ_a and the distance s along the contour are proportional to the chord, the additional velocity $v_a = \frac{d\Phi_a}{ds}$ will be independent of the chord.

The chord may then conveniently be chosen as that corresponding to a value $a = 1$ since a would then not appear in equations (10) and (12).

The net velocity at a point on the airfoil surface is the algebraic sum of the velocity on the isolated airfoil and the induced velocity v_a at that point.

Selection of vortices for source-vortex method.- For cascades of about unit solidity, the vortex distribution for an airfoil of conventional design may be represented by five vortices spaced on the mean line at 0.1, 0.3, 0.5, 0.7, and 0.9 of the chord. The strengths of the vortices are determined by the known chordwise distribution of potential Φ_T on the upper and lower surfaces for the given approximation. The difference in potential between the upper and lower surfaces at 0.2 chord is thus approximately the total vorticity between the leading edge and 0.2 chord and is considered to be concentrated in the vortex at 0.1 chord; similarly, the increase in this potential difference between 0.2 chord and 0.4 chord yields the strength of the vortex at 0.3 chord, and so on. The total vortex strength must satisfy the equation $\frac{\Gamma}{cV_0} = \frac{c_l}{2}$.

Selection of sources and sinks for source-vortex method.- The selection of sources and sinks to represent the thickness distribution of airfoils is less readily systematized than is the selection of vortices to represent the lift distribution. For conventional airfoils, a reasonably satisfactory representation is generally attainable with a source at about 0.025 chord, a second source midway between the nose and the position of maximum thickness, and sinks at 0.5, 0.7, and 0.9 of the chord. The strength of each source or sink is taken as the difference between the "internal flow" at a station midway between it and the preceding source, and the internal flow at a station midway between it and the following source. This internal flow at a given station is estimated to be the product of the thickness and the average of the upper and lower surface velocities at that station.

Obviously, not all airfoil shapes will be best treated according to the pattern just described; however, little ingenuity is required to adjust the treatment to a particular shape. In any case, the total source strength must equal the total sink strength.

PROCEDURE

A suggested step-by-step procedure is as follows:

(1) Obtain the velocities on the airfoil at the given angle of attack in a uniform stream by the method of reference 7. This step also determines a conformal correspondence between points (x, y) on the airfoil and angles φ on a circle, and hence the potential distribution Φ_f by equation (10).

(2) Using the procedure described in the section entitled "Computational Methods" choose sources, sinks, and vortices to represent the airfoil.

(3) Choose points around the airfoil at which the disturbance function W_d is to be found; these points are conveniently chosen, by reference to the conformal transformation, to correspond to 12 equal intervals about the circle. By use of figure 2, determine at these points the contributions to Φ_d and Ψ_d of each source and vortex row. Sum separately the values due to sources and vortices at each point.

(4) Form the compensating functions $\Psi_c = -\Psi_d$ both for vortices and sources and determine the conjugate functions by the method of reference 13. Plot Φ_c against φ and measure the slope at the trailing-edge point. The relation $\Gamma_a = -2\pi \left(\frac{d\Phi_c}{d\varphi}\right)_{T.E.}$ determines the circulation changes Γ_{a_s} and Γ_{a_v} due to the source and vortex rows. Obtain Γ_T by means of equation (1).

(5) At each point

(a) Sum the values of Φ_{d_v} and Φ_{c_v} due to the vortex rows and multiply by the ratio $\frac{\Gamma_T}{\Gamma_f}$.

(b) Sum the values of Φ_{d_s} and Φ_{c_s} due to the rows of sources and sinks.

(c) Find $\Phi_T = (\Gamma_T - \Gamma_f)\frac{\varphi}{2\pi}$.

(6) Sum the terms (a), (b), and (c) of step (5) to get Φ_a; plot Φ_a against the circle angle φ, and measure the slopes at the points used in the original conformal transformation (step (1)) at which points the stretching factor $\frac{d\varphi}{ds}$ will be known. The additional velocity is given by equation (11); the net velocity on the airfoil surface is the sum of the additional velocity and the velocity on the isolated airfoil. The corresponding total potential is $\Phi_T = \Phi_c + \Phi_d + \Phi_\Gamma + \Phi_f$, where Φ_f is known from step (1).

Using this new potential and velocity distribution, repeat the procedure, starting from step (2). The only modification is that Γ_T (step(4)) is now obtained from equation (2), and in step (5a) the correction factor is $\Gamma_{T_2}/\Gamma_{T_1}$. The process is continued until the changes in lift and velocity distribution become small. For practical purposes, the results obtained in this manner may be entirely satisfactory. More accurate results may be obtained, however, by application of the contour-integral method as described in the following three steps.

(7) Locate the points on the airfoil that correspond, by the conformal transformation, to points midway between those already located in step (3). Place the airfoil drawing on figure 2 with the origin, in turn, at each of the 12 points at which values are known from step (6) (considered as z-points), and read the chart at each of the 24 points (considered as z'-points). As previously noted, some of these points may be neglected. For each of the 24 (or fewer) points plot the 12 values of Φ read at that point against the 12 corresponding values of Φ_T. By planimetry find the area between the faired curve and the Φ_T-axis to determine Φ_d. The value of Ψ_d is determined similarly from a plot of the 12 values of Ψ against the corresponding values of Φ_T.

(8) Form the function $\Psi_c = -\Psi_d$, determine its conjugate Φ_c; the circulation change is $\Gamma_a = -2\pi\left(\frac{d\Phi_c}{d\varphi}\right)_{T.E.}$ and the potential $\Phi_\Gamma = \Gamma_a \frac{\varphi}{2\pi}$.

(9) Sum the terms Φ_c, Φ_d, and Φ_Γ to get Φ_a, plot against the circle angle φ, and measure the slopes. The velocities on the airfoil surface in cascade are obtained as described in step (6).

Unless this velocity distribution differs widely from that obtained in the preceding approximation, it should not be necessary to repeat the procedure.

The velocity distribution at another angle of attack may be obtained as follows:

(a) Solve equations (5) and (6) for θ_n, θ_t, and K. A method of solution is indicated in the discussion following equation (6). The angle of zero lift and slope of the lift curve may then be obtained from equations (7) and (8).

(b) Obtain the potential distribution Φ_ζ as a function of θ (equation (4)); compare with the known Φ_T to get a correspondence between θ and position on the airfoil. Equation (9) then yields the velocity distribution at stream angle λ_0'.

ILLUSTRATIVE EXAMPLES

Example 1.- The velocity distribution was obtained on the NACA 4412 airfoil in the configuration shown in figure 4, where $\beta = 0^\circ$, $\sigma = 1.032$, and $\lambda_0 = 9.7^\circ$. This example has been treated in reference 8. In accordance with the foregoing procedure, results as follows were obtained:

(1) In figure 5 is shown the chordwise velocity distributions of the isolated airfoil at the angle of attack of 9.7°, as obtained in a second approximation by the method of reference 7. The lift coefficient at this angle of attack is 1.67 (that is, $\frac{\Gamma_f}{cV_0} = 0.837$), the angle of zero lift of the airfoil is -4.24°, and the slope of the lift curve is 6.95 per radian.

(2) By use of the procedure suggested in the section entitled "Computational Methods," five vortices, two sources, and three sinks were chosen to represent the airfoil initially (fig. 6 and table I).

(3) With the first location at the trailing edge, 12 locations on the airfoil were found corresponding to 30° intervals of the circle angle φ. These locations are shown in figure 6. (The primed points correspond to 15° intervals.) Readings taken at these points from figure 2 are given in table II. These readings, multiplied by the appropriate source and vortex strengths, yielded the values of Φ_d and Ψ_d due to sources and vortices given in table III.

(4) The conjugate functions Φ_c were determined by the 12-point method and are given in table IV. The slopes of these functions at the trailing-edge point yielded circulation changes $\frac{\Gamma_{a_s}}{cV_0} = 0.006$ and $\frac{\Gamma_{a_v}}{cV_0} = -0.538$, from which (equation (1))

$\frac{\Gamma_T}{cV_0} = 0.513$. This value corresponds to a first approximate lift coefficient in cascade $(c_l = 1.03)$.

(5) In table IV are given the values of Φ_{c_v} and Φ_{d_v} due to vortex rows multiplied by the ratio $\frac{\Gamma_T}{\Gamma_f}$ (equation (1)), the values of Φ_{c_s} and Φ_{d_s} due to source rows, and the function

$$\Phi_\Gamma = (\Gamma_T - \Gamma_f)\frac{\varphi}{2\pi}.$$

(6) The additional potential $\Phi_a = \Phi_d + \Phi_c + \Phi_\Gamma$ is plotted in figure 7. Slopes of this function were measured at points at which the stretching factor is known from step (1). The additional velocity v_a was then computed by equation (10); the algebraic sum of v_a and the velocity in isolated flow yielded the cascade velocity (fig. 5). This velocity distribution, together with the total potential Φ_T, formed the basis for a second approximation (figs. 5 and 7). Results of this approximation are $\frac{\Gamma_{a_s}}{cV_0} = 0.006$, $\frac{\Gamma_{a_v}}{cV_0} = -0.365$, and $c_l = 0.99$. Comparison of the velocity distribution with that of the first approximation shows that the process has satisfactorily converged.

(7) The same 12 points around the airfoil were chosen as z-points; these, together with four others at 15° intervals around the nose (primed points in fig. 6) were used as z'-points. Readings from the chart (fig. 2) are given in table V. These values were plotted against total potential Φ_T (arbitrarily fixed at 0 on the lower surface at the trailing edge). (A sample curve is shown in fig. 8.) These curves were integrated by planimetry. The results - the disturbance potentials and stream functions Φ_d and Ψ_d - are given in table VI.

(8) The function Φ_c (table VI) was obtained by 24-point harmonic analysis and synthesis, with the use of interpolated values of Ψ_c for the points at which it was not found explicitly. The slope of the curve at the trailing-edge point yielded $\frac{\Gamma_a}{cV_0} = -0.344$, from which a lift coefficient $c_l = 0.99$ was obtained.

(9) The additional potential $\Phi_a = \Phi_d + \Phi_c + \Phi_\Gamma$ is plotted in figure 7. The velocity distribution was obtained as before and is plotted in figure 5. The process appears to have essentially converged.

Simultaneous solution of equations (5) and (6) (table VII) to find the value of K at which $\frac{\Delta\Phi_\zeta}{cV_0} = \frac{\Delta\Phi_T}{cV_0}$ gave $K = 0.3083$, $\theta_n = -7.57^\circ$, and $\theta_t = 181.72^\circ$. Equations (7) and (8) then yielded the angle of zero lift $\eta = -5.75^\circ$ and the slope of the lift curve $\frac{dc_l}{d\alpha_0} = 3.71$. These values may be compared with $\eta = -5.94^\circ$ and $\frac{dc_l}{d\alpha_0} = 3.71$ from reference 8.

In figure 9 is shown a plot of the potential Φ_ζ against θ computed by equation (4). A constant has been added to make the potential equal to zero on the lower surface at the trailing edge. The known total potential in cascade Φ_T and the corresponding values of x/c are given in table VIII. Values of θ, picked off the plot at points where Φ_ζ is equal to the given values of Φ_T, are shown in the adjacent column. The correspondence between airfoil position and the angle θ is thus determined. For the flow angles $\lambda_0' = 1.81^\circ$ and $\lambda_0' = -5.94^\circ$, the velocity distributions were computed by equation (9). In figure 10 these results are compared with the distributions given in reference 8. The main results of the calculations are summarized in table IX.

Example II.- In an effort to obtain in the simplest possible manner a reference solution at large blade angle, concerning the accuracy of which there could be little doubt, a lattice was derived by a modified Joukowski transformation. This transformation is discussed in detail in the appendix. The cascade configuration is shown in figure 11 where $\beta = 45^\circ$, $\sigma = 1.006$, and $\lambda_0 = 49^\circ$. This lattice will be referred to as the "derived airfoil lattice."

The procedure followed for the source-vortex method was similar to that of the first example; the calculations are outlined in figures 12 to 14. Because of the unusual shape of this profile, only one source was used and an additional sink was inserted at 0.3 chord (fig. 12). From a lift coefficient $c_l = 0.84$ in isolated flow, a single approximation yielded a lift coefficient $c_l = 0.54$ in cascade, which was the same as that derived from the solution by conformal transformation. Since the computed changes in vortex distribution were small, no further approximations were made by this method. By reference to the velocity distribution of this approximation (fig. 13), the process may be seen to have essentially converged to the correct solution.

The final contour integration resulted in a lift coefficient $c_l = 0.54$ and the velocity distribution shown in figure 13. The main results of the calculations are summarized in table X.

Langley Memorial Aeronautical Laboratory
National Advisory Committee for Aeronautics
Langley Field, Va., January 10, 1947

APPENDIX

DERIVED AIRFOIL LATTICE

The symbols used in the appendix are defined in figure 15 and should not be confused with similar symbols used in the main text of the paper.

Consider the transformation (reference 10),

$$z = \frac{1}{2\pi}\left(e^{-i\beta}\log_e\frac{\zeta + e^{K}}{\zeta - e^{K}} + e^{i\beta}\log_e\frac{\zeta + e^{-K}}{\zeta - e^{-K}}\right) \tag{A1}$$

The unit circle (ζ-plane) becomes a lattice of horizontal straight lines in the z-plane, spaced at unit intervals along the stagger line, making an angle $\frac{\pi}{2} - \beta$ with the axis of reals. The solidity of this lattice is

$$\sigma = \frac{2}{\pi}\left(\cos\beta\log_e\frac{\sqrt{\sinh^2 K + \cos^2\beta} + \cos\beta}{\sinh K} + \sin\beta\tan^{-1}\frac{\sin\beta}{\sqrt{\sinh^2 K + \cos^2\beta}}\right)$$

This relation is plotted in figure 3.

A closed curve enclosing the points $\zeta = \pm e^{-K}$ but not enclosing the points $\zeta = \pm e^{K}$ will transform by equation (A1) into an infinite lattice of closed shapes in the z-plane, spaced in the same manner as the straight-line lattice. Such a curve is the circle

$$\begin{aligned}\zeta &= e^{\psi + i\theta} \\ &= e^{\psi_0 + i\phi} + re^{i\delta} \\ &= 1.07e^{i\phi} + 0.09e^{-\frac{i\pi}{3.75}}\end{aligned}$$

This circle, where $\beta = 45^\circ$ and $K = 0.331$, becomes the lattice of profiles that has been referred to as the derived airfoil lattice. A flow for which this circle is a streamline and which, in the z-plane, has no singularities outside the profiles, is that due to the system of sources, sinks, and vortices shown in figure 15. The velocity on the circle boundary due to this system is

$$\left(\frac{v}{V_0}\right)_\zeta = A \cos \lambda_0 + B \sin \lambda_0 + C\frac{\Gamma}{2V_0}$$

where

$$A = e^{-\psi_0}\left[\frac{\sin(\phi - \delta_1)}{H_1 - \cos(\phi - \delta_1)} - \frac{\sin(\phi - \delta_2)}{H_2 - \cos(\phi - \delta_2)}\right]$$

$$B = e^{-\psi_0}\left[\frac{J_1}{H_1 - \cos(\phi - \delta_1)} - \frac{J_2}{H_2 - \cos(\phi - \delta_2)}\right]$$

$$C = e^{-\psi_0}\left[\frac{J_1}{H_1 - \cos(\phi - \delta_1)} + \frac{J_2}{H_2 - \cos(\phi - \delta_2)}\right]$$

and

$$\delta_1 = \tan^{-1}\frac{r \sin \delta}{e^K - r \cos \delta} \qquad \delta_2 = \tan^{-1}\frac{-r \sin \delta}{e^K + r \cos \delta}$$

$$H = \frac{1}{2}\left(m + \frac{1}{m}\right) \qquad J = \frac{1}{2}\left(\frac{1}{m} - m\right)$$

$$m_1 = e^{-\psi_0}\sqrt{r^2 + e^{2K} - 2re^K \cos \delta} \qquad m_2 = e^{-\psi_0}\sqrt{r^2 + e^{2K} + 2re^K \cos \delta}$$

The constant Γ which is the circulation about each profile (positive clockwise), is determined by the trailing-edge condition as

$$\frac{\Gamma}{V_0} = -2\left(\frac{A}{C} \cos \lambda_0 + \frac{B}{C} \sin \lambda_0\right) \qquad (A2)$$

where A, B, and C are evaluated at the angle ϕ which corresponds to the trailing edge of the profile. The angle of zero lift η with respect to the airfoil chord, is obtained from equation (A2) by setting $\Gamma = 0$; thus,

$$\eta = -\tan^{-1}\frac{A}{B} - \beta$$

The stretching factor from the circle to the lattice is

$$\left|\frac{d\zeta}{dz}\right| = \frac{e^{-\psi}}{2}\sqrt{\frac{D}{E}}$$

where

$$D = \left[(\cosh 2K - \cosh 2\psi \cos 2\theta)^2 + (\sinh 2\psi \sin 2\theta)^2\right]$$

$$E = \Big[4 \cos^2\beta \cosh^2 K(\cosh^2\psi - \cos^2\theta) + 4 \sin^2\beta \sinh^2 K(\cosh^2\psi - \sin^2\theta) - \sin 2\beta \sin 2\theta \sinh 2K\Big]$$

and ψ and θ are obtained from ψ_0, ϕ, r, and δ as

$$\theta = \tan^{-1}\frac{e^{\psi_0}\sin\phi + r \sin\delta}{e^{\psi_0}\cos\phi + r\cos\delta}$$

$$e^{\psi} = r\cos(\theta - \delta) + \sqrt{e^{2\psi_0} - r^2\sin^2(\theta - \delta)}$$

The velocity at any point on the surface of a profile is

$$\left(\frac{v}{V_0}\right)_z = \left(\frac{v}{V_0}\right)_\zeta \left|\frac{d\zeta}{dz}\right|$$

REFERENCES

1. Betz, Albert: Diagrams for Calculation of Airfoil Lattices. NACA TM No. 1022, 1942.

2. Pistolesi, E.: On the Calculation of Flow past an Infinite Screen of Thin Airfoils. NACA TM No. 968, 1941.

3. Pistolesi, E., and Toniolo, A.: Sul calcolo pratico delle schiere alari. L'Aerotecnica, vol. 18, fasc. 10, Oct. 1938, pp. 1065-1094.

4. Collar, A. R.: The Flow of a Perfect Fluid through Cascades of Aerofoils. Jour. R.A.S., vol. XLV, no. 365, May 1941, pp. 183-213.

5. Merchant, W., and Collar, A. R.: Flow of an Ideal Fluid past a Cascade of Blades (Part II). R. & M. No. 1893, British A.R.C., 1941.

6. Howell, A. R.: Note on the Theory of Arbitrary Aerofoils in Cascade. Note No. E.3859, British R.A.E., March 1941.

7. Theodorsen, T., and Garrick, I. E.: General Potential Theory of Arbitrary Wing Sections. NACA Rep. No. 452, 1933.

8. Garrick, I. E.: On the Plane Potential Flow past a Lattice of Arbitrary Airfoils. NACA ARR No. 4A07, 1944.

9. Mutterperl, William: A Solution of the Direct and Inverse Potential Problems for Arbitrary Cascades of Airfoils. NACA ARR No. L4K22b, 1944.

10. von Kármán, Th., and Burgers, J. M.: General Aerodynamic Theory - Perfect Fluids. Application of the Theory of Conformal Transformation to the Investigation of the Flow around Airfoil Profiles. Vol. II of Aerodynamic Theory, div. E, ch. II, pt. B, W. F. Durand, ed., Julius Springer (Berlin), 1935, pp. 91-96.

11. Weinig, F.: Die Strömung um die Schaufeln von Turbomaschinen. Johann Ambrosius Barth (Leipzig), 1935.

12. von Mises, Richard: The Theory of Flight. McGraw-Hill Book Co., Inc., 1945, p. 198.

13. Naiman, Irven: Numerical Evaluation by Harmonic Analysis of the ϵ-Function of the Theodorsen Arbitrary-Airfoil Potential Theory. NACA ARR No. L5H18, 1945.

14. Theodorsen, Theodore: Airfoil-Contour Modifications Based on ϵ-Curve Method of Calculating Pressure Distribution. NACA ARR No. L4G05, 1944.

TABLE I

STRENGTHS OF SOURCES AND VORTICES CHOSEN TO REPRESENT

THE NACA 4412 AIRFOIL LATTICE

Vortex location (fig. 6)	$\frac{\gamma}{cV_0}$		Source location (fig. 6)	$\frac{m}{cV_0}$	
	First approximation	Second approximation		First approximation	Second approximation
β	0.379	0.290	α	0.097	0.101
δ	.184	.098	γ	.044	.044
ϵ	.128	.062	ϵ	-.043	-.041
ζ	.097	.042	ζ	-.045	-.047
η	.052	.023	η	-.053	-.057

NATIONAL ADVISORY
COMMITTEE FOR AERONAUTICS

TABLE II

CHART READINGS FOR NACA 4412 AIRFOIL LATTICE, SOURCE-VORTEX METHOD

	Φ for vortex row of unit strength							Ψ for vortex row of unit strength						
Origin at (fig. 6)- / Reading at (fig. 6)-	.7 α	.311 β	+.041 γ	.184 δ	.126 −.043 ε	.047 −.046 ζ	.052 −.053 η	+.077 α	.211 β	+.044 γ	.186 δ	.123 −.043 ε	.07 −.046 ζ	.029 −.053 η
a	0.002	0.008	0.008	0.011	0.010	0.004	0.001	-0.211	-0.184	-0.176	-0.120	-0.070	-0.025	-0.003
b	.002	.008	.008	.011	.010	.003	0	-.182	-.158	-.150	-.096	-.047	-.013	0
c	.004	.008	.008	.009	.005	-.001	-.002	-.115	-.092	-.083	-.044	-.011	0	-.010
d	.005	.006	.006	.004	-.002	-.007	-.007	-.045	-.030	-.026	-.004	0	-.019	-.056
e	.002	.002	.002	-.004	-.012	-.013	-.013	-.007	-.001	0.	-.002	-.025	-.040	-.125
f	0	-.001	-.002	-.008	-.015	-.013	-.011	0	-.001	-.001	-.019	-.057	-.115	-.174
g	0	0	0	-.003	-.005	-.002	0	0	-.003	-.002	-.024	-.063	-.120	-.183
h	-.002	0	.001	.002	.005	.010	.016	0	.001	0	-.012	-.044	-.090	-.156
i	-.012	-.007	-.006	.001	.008	.015	.023	-.014	-.006	-.004	.001	-.013	-.048	-.098
j	-.020	-.015	-.014	-.006	0	.010	.016	-.058	-.042	-.037	-.010	.001	-.010	-.042
k	-.016	-.011	-.010	-.005	.002	0	.004	-.125	-.102	-.094	-.050	-.018	0	-.006
l	-.005	0	0	.005	.004	.001	0	-.185	-.161	-.153	-.097	-.048	-.015	0

NATIONAL ADVISORY
COMMITTEE FOR AERONAUTICS

TABLE III

CONTRIBUTIONS OF INDIVIDUAL SOURCE AND VORTEX ROWS TO THE DISTURBANCE FLOW FUNCTION ON THE NACA 4412 AIRFOIL IN CASCADE; FIRST APPROXIMATION, SOURCE-VORTEX METHOD

Point of Reading at (fig. 6)	β	δ	ϵ	ζ	η	α	γ	ϵ	ξ	η
	Φ_d due to vortex rows					Φ_d due to source rows				
a	0.0030	0.0020	0.0013	0.0004	0	0.0205	0.0077	-0.0030	-0.0011	-0.0001
b	.0030	.0020	.0013	.0003	0	.0176	.0066	-.0020	-.0006	0
c	.0030	.0016	.0006	-.0001	-.0001	.0112	.0036	-.0005	0	-.0005
d	.0023	.0007	-.0002	-.0007	-.0004	.0044	.0011	0	-.0008	-.0030
e	.0008	-.0007	-.0015	-.0013	-.0007	.0007	0	-.0011	-.0018	-.0065
f	-.0004	-.0015	-.0019	-.0013	-.0006	0	.0001	-.0024	-.0052	-.0092
g	0	-.0006	-.0006	-.0002	0	0	.0001	-.0027	-.0054	-.0097
h	0	.0005	.0006	.0010	.0008	0	0	-.0019	-.0040	-.0083
i	-.0026	.0002	.0010	.0014	.0012	.0014	.0002	-.0006	-.0022	-.0052
j	-.0057	-.0011	0	.0010	.0008	.0056	.0016	0	-.0004	-.0022
k	-.0042	-.0009	.0003	0	.0002	.0121	.0041	-.0008	0	-.0003
l	0	.0009	.0005	.0001	0	.0180	.0067	-.0021	-.0007	0
	Ψ_d due to vortex rows					Ψ_d due to source rows				
a	-0.0698	-0.0221	-0.0090	-0.0024	-0.0001	0.0002	0.0004	-0.0004	-0.0002	0
b	-.0599	-.0176	-.0060	-.0013	0	.0002	.0004	-.0004	-.0001	0
c	-.0348	-.0081	-.0014	0	-.0005	.0004	.0004	-.0002	0	.0001
d	-.0114	-.0007	0	-.0018	-.0029	.0005	.0003	.0001	.0003	.0004
e	-.0005	-.0005	-.0032	-.0039	-.0065	.0002	.0001	.0005	.0006	.0007
f	-.0003	-.0035	-.0073	-.0111	-.0091	0	.0001	.0006	.0006	.0006
g	-.0010	-.0044	-.0081	-.0116	-.0096	0	0	.0002	.0001	0
h	.0002	-.0021	-.0056	-.0087	-.0081	-.0002	0	-.0002	-.0004	-.0008
i	-.0023	-.0002	-.0017	-.0046	-.0051	-.0012	-.0003	-.0003	-.0007	-.0012
j	-.1057	-.0018	.0001	-.0009	-.0022	-.0019	-.0006	0	-.0004	-.0008
k	-.0386	-.0092	-.0022	0	-.0003	-.0016	-.0004	-.0001	0	-.0002
l	-.0610	-.0178	-.0061	-.0014	0	-.0005	0	-.0002	0	0

TABLE IV

TOTAL EFFECT OF SOURCE AND VORTEX ROWS, AND CORRESPONDING DERIVED POTENTIALS AND VELOCITIES, ON NACA 4412 AIRFOIL IN CASCADE; FIRST APPROXIMATION, SOURCE-VORTEX METHOD

Point	Values at points on figure 6											Values at points where $\frac{d\varphi}{ds}$ is known					
	1	2	3	4	5	6	7	8	9	10	11						
	$\frac{\Psi_d}{cV_0}$	$\frac{\Phi_c}{cV_0}$	$\frac{\Phi_d}{cV_0}$	$\frac{\Psi_a}{cV_0}$	$\frac{\Phi_e}{cV_0}$	$\frac{\Phi_f}{cV_0}$	$\frac{\Phi_{dw}+\Phi_{ad}}{cV_0}\frac{\Gamma_{T_1}}{\Gamma_f}$	$\frac{\Phi_T}{cV_0}$	$\frac{\Phi_a}{cV_0}$	$\frac{\Phi_f}{cV_0}$	$\frac{\Phi_T}{cV_0}$	$\frac{x}{c}$	$\frac{1}{cV_0}\frac{d\Phi_a}{d\varphi}$	$\frac{c\,d\varphi}{ds}$	$\frac{v_a}{V_0}$ (a)	$\frac{v_f}{V_0}$ (a)	$\frac{v_T}{V_0}$ (a)
	Sources			Vortices								Upper surface					
a	0.0000	0.0014	0.0240	-0.1034	0.0013	0.0067	0.0049	-0.0270	0.0033	0.6056	0.6089						
b	.0001	.0014	.0216	-.0848	.0414	.0066	.0295	-.0540	-.0015	.5355	.5340	0.0125	-0.0356	7.153	-0.254	2.287	2.033
c	.0007	.0015	.0138	-.0448	.0513	.0050	.0347	-.0810	-.0310	.3592	.3282	.0500	-.0427	4.541	-.194	2.002	1.808
d	.0016	.0009	.0017	-.0168	.0314	.0017	.0206	-.1080	-.0848	.1429	.0581	.1000	-.0456	3.500	-.160	1.853	1.693
e	.0021	-.0003	-.0097	-.0146	.0040	-.0034	.0004	-.1350	-.1436	-.0365	-.1801	.2000	-.0542	2.733	-.148	1.719	1.571
f	.0019	-.0020	-.0167	-.0313	-.0050	-.0057	-.0065	-.1620	-.1872	-.1126	-.2998	.4000	-.0606	2.218	-.140	1.523	1.383
g	.0003	-.0030	-.0177	-.0347	.0037	-.0014	.0014	-.1891	-.2084	-.0459	-.2543	.6000	-.0506	2.133	-.108	1.345	1.237
h	-.0016	-.0032	-.0142	-.0243	.0044	.0029	.0045	-.2161	-.2290	.1642	-.0648	.8000	-.0226	2.498	-.057	1.178	1.121
i	-.0037	-.0018	-.0064	-.0139	-.0098	.0012	-.0053	-.2431	-.2566	.4802	.2236	.9000	-.0078	3.226	-.025	1.078	1.053
j	-.0037	.0007	.0046	-.0205	-.0356	-.0030	-.0236	-.2701	-.2884	.8365	.5481	Lower surface					
k	-.0023	.0022	.0151	-.0503	-.0505	-.0046	-.0338	-.2971	-.3136	1.1558	.8422	0.0125	-0.0451	8.263	-0.372	0.458	0.086
l	-.0007	.0022	.0219	-.0863	-.0372	.0015	-.0218	-.3241	-.3218	1.3716	1.0498	.0500	-.0651	4.603	-.300	-.314	-.614
a	.0000	.0014	.0240	-.1034	.0013	.0067	.0049	-.3511	-.3208	1.4451	1.1243	.1000	-.0847	3.304	-.280	-.541	-.821
												.2000	-.1027	2.413	-.248	-.676	-.924
												.4000	-.1157	1.914	-.221	-.754	-.975
												.6000	-.1008	1.903	-.192	-.796	-.988
												.8000	-.0621	2.335	-.145	-.834	-.979
												.9000	-.0328	3.080	-.101	-.845	-.946

[a] Velocities along the surface are considered positive when directed from the lower surface at the trailing edge toward the upper surface at the trailing edge.

NATIONAL ADVISORY COMMITTEE FOR AERONAUTICS

TABLE V

CHART READINGS FOR INTEGRATION WITH RESPECT TO Φ_T; NACA 4412 AIRFOIL IN CASCADE; CONTOUR-INTEGRAL METHOD

z' \ z	a	b	c	d	e	f	g	h	i	j	k	l
$\Phi_T \rightarrow$	[a]1.0818 / [b]0.5875	0.5400	0.3106	0.0401	-0.2022	-0.3280	-0.2911	-0.1064	0.1783	0.4986	0.7954	1.0060
	Φ											
a	0	0	-0.001	-0.0040	-0.0095	-0.008	0.004	0.020	0.029	0.0215	0.008	0.001
b	0	0	0	-.003	-.0085	-.006	.005	.021	.0275	.020	.0065	0
c	-.0005	0	0	-.0015	-.006	-.005	.006	.0195	.0215	.0105	-.0005	-.003
d	-.0045	-.003	-.0015	0	-.0015	-.001	.0065	.0145	.010	-.0035	-.0125	-.009
e	-.010	-.008	-.006	-.0015	0	.0005	.004	.0055	.006	-.0205	-.023	-.016
e'	-.011	-.010	-.007	-.002	0	0	.0025	0	-.012	-.025	-.026	-.018
f	-.009	-.008	-.005	-.001	.0005	0	.0005	-.0025	-.014	-.026	-.025	-.014
f'	-.002	-.001	0	.002	.002	0	0	-.0035	-.014	-.024	-.0215	-.010
g	.007	.007	.0065	.0065	.0045	0	0	-.002	-.010	-.018	-.015	-.002
g'	.015	.015	.012	.011	.0055	0	0	-.0005	-.0065	-.0125	-.008	.006
h	.024	.022	.019	.0145	.0050	-.0035	-.003	0	-.0025	-.006	.0005	.015
h'	.028	.027	.022	.014	.001	-.008	-.0065	.001	-.0005	-.0015	.0055	.0195
i	.0295	.0285	.022	.0095	-.006	-.0155	-.0115	.003	0	.0005	.008	.0215
j	.022	.020	.0105	.0050	-.0205	-.027	-.0185	.006	0	0	.0035	.016
k	.008	.0065	-.0015	-.012	-.023	-.025	-.014	-.0005	.008	.0035	0	.004
l	.001	0	-.003	-.0085	-.015	-.017	-.001	-.015	.021	.0155	.004	0
	Ψ											
a	0	-0.002	-0.024	-0.083	-0.154	-0.205	-0.217	-0.186	-0.130	-0.066	-0.018	-0.002
b	-.002	0	-.012	-.063	-.132	-.178	-.187	-.159	-.102	-.045	-.0075	0
c	-.023	-.012	0	-.0205	-.073	-.111	-.120	-.095	-.048	-.0085	.001	-.0125
d	-.081	-.060	-.0205	0	-.018	-.042	-.048	-.030	-.004	.0025	-.023	-.062
e	-.153	-.128	-.070	-.0175	0	-.006	-.0075	0	.002	-.023	-.077	-.131
e'	-.184	-.157	-.091	-.031	-.003	-.0005	-.0015	.002	-.0035	-.040	-.100	-.159
f	-.204	-.180	-.109	-.042	-.007	0	0	.0015	-.011	-.053	-.119	-.181
f'	-.214	-.189	-.119	-.048	-.0085	0	0	-.001	-.017	-.064	-.129	-.191
g	-.212	-.186	-.116	-.047	-.008	0	0	-.0015	-.0175	-.063	-.128	-.189
g'	-.205	-.176	-.110	-.0415	-.005	.0015	0	-.001	-.0145	-.056	-.120	-.181
h	-.184	-.158	-.093	-.030	0	.0015	-.0015	0	-.008	-.044	-.103	-.160
h'	-.158	-.133	-.073	-.017	.0035	-.002	-.006	-.002	-.003	-.0295	-.082	-.136
i	-.127	-.101	-.048	-.0035	.0025	-.011	-.017	-.0085	0	-.015	-.058	-.105
j	-.062	-.044	-.008	.003	-.0225	-.054	-.063	-.044	-.0155	0	-.016	-.047
k	-.018	-.0075	.001	-.012	-.081	-.123	-.130	-.103	-.059	-.016	0	-.0085
l	-.002	0	-.013	-.009	-.131	-.079	-.188	-.164	-.108	-.0475	-.009	0

[a]Upper surface at trailing edge.

[b]Lower surface at trailing edge.

NATIONAL ADVISORY
COMMITTEE FOR AERONAUTICS

TABLE VI

DERIVED POTENTIALS AND VELOCITIES ON NACA 4412 AIRFOIL IN CASCADE;

CONTOUR-INTEGRAL METHOD

Values at points on figure 6								Values where $\frac{d\varphi}{ds}$ is known					
z'	$\frac{\Phi_d}{cV_0}$	$\frac{\Psi_d}{cV_0}$	$\frac{\Phi_c}{cV_0}$	$\frac{\Phi_T}{cV_0}$	$\frac{\Phi_a}{cV_0}$	$\frac{\Phi_f}{cV_0}$	$\frac{\Psi_T}{cV_0}$	$\frac{x}{c}$	$\frac{l}{cV_0}\frac{d\Phi_a}{d\varphi}$	$\frac{cd\varphi}{ds}$	$\frac{V_a}{V_0}$ (a)	$\frac{V_f}{V_0}$ (a)	$\frac{V_T}{V_0}$ (a)
a	0.0281	-0.0687	0.0021	-0.0144	0.0158	0.5717	0.5875	Upper surface					
b	.0259	-.0571	.0271	-.0432	.0098	.5302	.5400	0.0125	-0.0403	7.153	-0.288	2.287	1.999
c	.0164	-.0314	.0382	-.0720	-.0174	.3280	.3106	.0500	-.0496	4.541	-.225	2.002	1.777
d	.0033	-.0098	.0257	-.1008	-.0718	.1119	.0401	.1000	-.0525	3.500	-.184	1.853	1.669
e	-.0129	-.0049	.0090	-.1296	-.1335	-.0687	-.2022	.2000	-.0667	2.733	-.182	1.719	1.537
e'	-.0184	-.0071	.0017	-.1440	-.1607	-.1237	-.2844	.4000	-.0650	2.218	-.144	1.523	1.379
f	-.0219	-.0114	-.0012	-.1584	-.1815	-.1465	-.3280	.6000	-.0452	2.133	-.096	1.345	1.249
f'	-.0210	-.0130	-.0031	-.1728	-.1969	-.1329	-.3298	.8000	-.0189	2.498	-.047	1.178	1.131
g	-.0186	-.0164	-.0035	-.1872	-.2093	-.0818	-.2911	.9000	-.0042	3.226	-.014	1.078	1.064
g'	-.0157	-.0151	-.0015	-.2017	-.2189	.0060	-.2129	Lower surface					
h	-.0128	-.0128	-.0043	-.2161	-.2332	.1268	-.1064	0.0125	-0.0598	8.263	-0.494	0.458	-0.036
h'	-.0096	-.0118	-.0066	-.2305	-.2467	.2747	.0280	.0500	-.0792	4.603	-.364	-.314	-.678
i	-.0071	-.0092	-.0122	-.2449	-.2642	.4425	.1783	.1000	-.0938	3.304	-.310	-.541	-.851
j	.0002	-.0187	-.0261	-.2737	-.2996	.7982	.4986	.2000	-.1078	2.413	-.260	-.676	-.936
k	.0115	-.0362	-.0323	-.3025	-.3233	1.1187	.7954	.4000	-.1199	1.914	-.230	-.754	-.984
l	.0232	-.0586	-.0224	-.3313	-.3305	1.3365	1.0060	.6000	-.1073	1.903	-.203	-.796	-.999
a	.0281	-.0687	.0021	-.3601	-.3299	1.4117	1.0818	.8000	-.0564	2.335	-.132	-.834	-.966
								.9000	-.0333	3.080	-.103	-.845	-.948

[a] Velocities along the surface are considered positive when directed from the trailing edge to the leading edge on the lower surface, and from the leading edge to the trailing edge on the upper surface.

NATIONAL ADVISORY
COMMITTEE FOR AERONAUTICS

TABLE VII

COMPUTATION OF MAPPING FUNCTION CONSTANTS

FOR NACA 4412 AIRFOIL LATTICE

K	θ_n (deg)	θ_t (deg)	S	T	U	$\frac{\Delta\Phi_\zeta}{cV_0}$
0.3	-7.37	181.62	1.1307	0.0157	0.2879	1.4343
0.4	-9.81	182.38	.9585	.0152	.2895	1.2632
0.32	-7.85	181.83	1.0920	.0156	.2886	1.3962
0.311	-7.63	181.73	1.1088	.0157	.2882	1.4127
0.308	-7.57	181.72	1.1147	.0157	.2882	1.4186
0.309	-7.59	181.73	1.1128	.0157	.2882	1.4167
0.3083	-7.57	181.72	1.1144	.0157	.2882	1.4183 $\left(= \frac{\Delta\Phi_T}{cV_0}\right)$

$$S = \frac{\cos \lambda_0}{2\pi\sigma} \log_e \left[\frac{(\cosh K - \cos \theta_t)(\cosh K + \cos \theta_n)}{(\cosh K + \cos \theta_t)(\cosh K - \cos \theta_n)} \right]$$

$$T = \frac{\sin \lambda_0}{\pi\sigma} \tan^{-1} \left[\frac{(\sin \theta_n - \sin \theta_t)\sinh K}{\sinh^2 K + \sin \theta_n \sin \theta_t} \right]$$

$$U = \frac{T}{2\pi c V_0} \tan^{-1} \left[\frac{(\tan \theta_n - \tan \theta_t)\tanh K}{\tanh^2 K + \tan \theta_n \tan \theta_t} \right]$$

TABLE VIII

RELATION BETWEEN CIRCLE ANGLE θ (ζ-PLANE) AND LOCATION ON NACA 4412 AIRFOIL IN CASCADE

Upper surface				Lower surface			
Point	Φ_T/cV_0	x/c	θ (deg)	Point	Φ_T/cV_0	x/c	θ (deg)
g	-0.2911	0.006	1.4	a	0.5875	1.000	-178.3
h	-.1064	.090	17.0	b	.5400	.920	-167.3
i	.1783	.270	45.7	c	.3106	.707	-135.8
j	.4986	.501	98.6	d	.0401	.435	-82.9
k	.7954	.740	145.2	e	-.2022	.187	-35.1
l	1.0060	.927	168.2	f	-.3280	.033	-11.8

NATIONAL ADVISORY
COMMITTEE FOR AERONAUTICS

TABLE IX

CONSTANTS OF NACA 4412 AIRFOIL LATTICE

	Source-vortex method		Contour-integral method	Method of reference 8
	First approximation	Second approximation		
$\Delta\Gamma_s/cV_0$	0.006	0.006	----------	----------
$\Delta\Gamma_v/cV_0$	-.538	-.365	----------	----------
$\Delta\Gamma_a/cV_0$	-.324	-.342	-0.346	----------
c_l	1.03	.99	.99	1.00
$\bar{K}$	----------	----------	.3083	.3109
θ_t, deg	----------	----------	181.73	181.79
$dc_l/d\alpha_0$	----------	----------	3.71	3.71
η, deg	----------	----------	-5.75	-5.94

NATIONAL ADVISORY
COMMITTEE FOR AERONAUTICS

TABLE X

CONSTANTS OF DERIVED AIRFOIL LATTICE

	Source-vortex method; first approximation	Contour-integral method	Conformal transformation
$\Delta\Gamma_s/cV_0$	-0.083	----------	----------
$\Delta\Gamma_v/cV_0$	-.101	----------	----------
$\Delta\Gamma_a/cV_0$	-.148	-0.152	----------
c_l	.54	.54	0.54
K	----------	.2637	.2635
θ_t,deg	----------	193.50	193.46
$dc_l/d\alpha_0$	----------	5.11	5.11
η,deg	----------	-2.03	-2.11

NATIONAL ADVISORY
COMMITTEE FOR AERONAUTICS

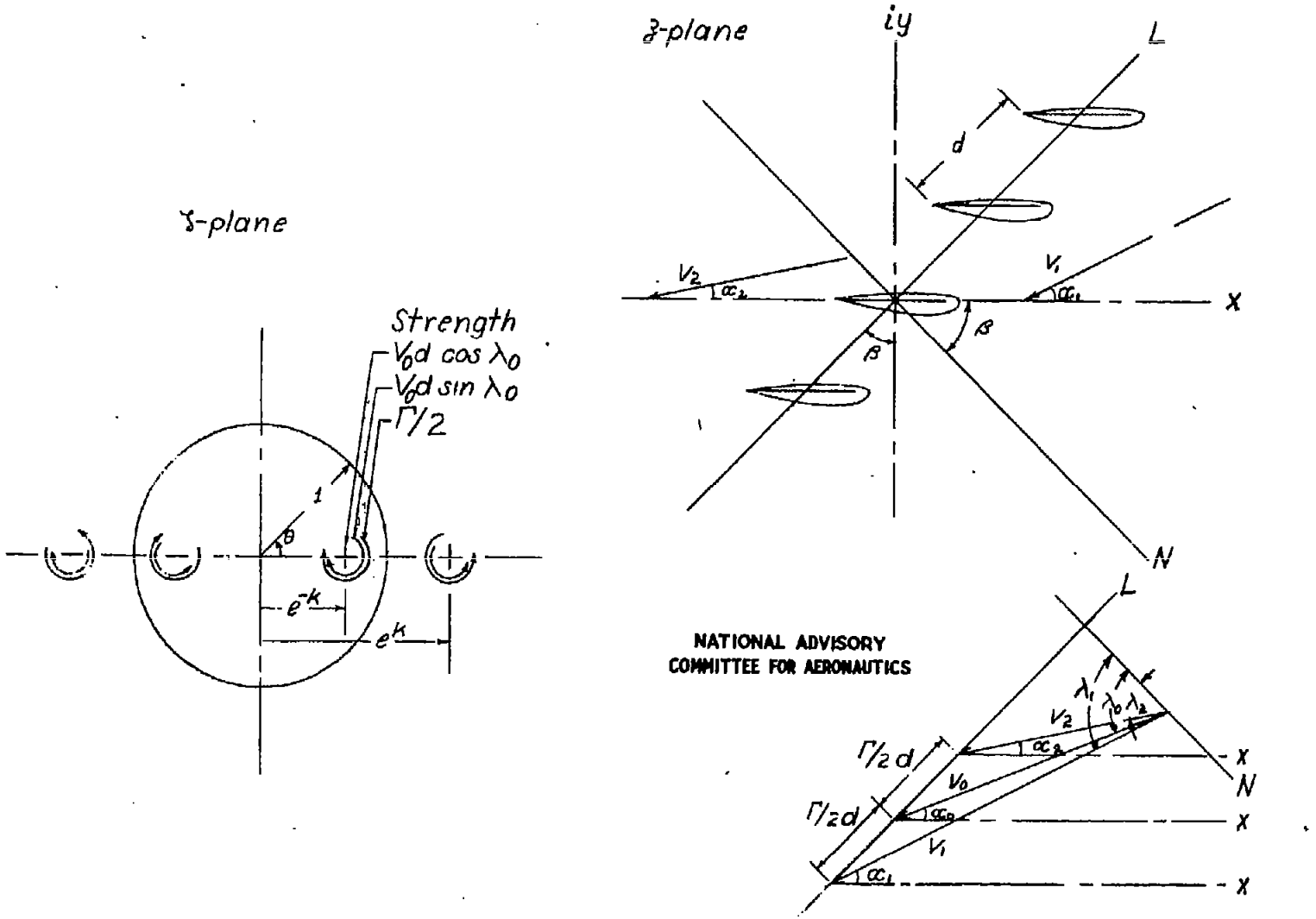

Figure 1 .—Flow singularities in circle plane and corresponding velocity vectors in physical plane.

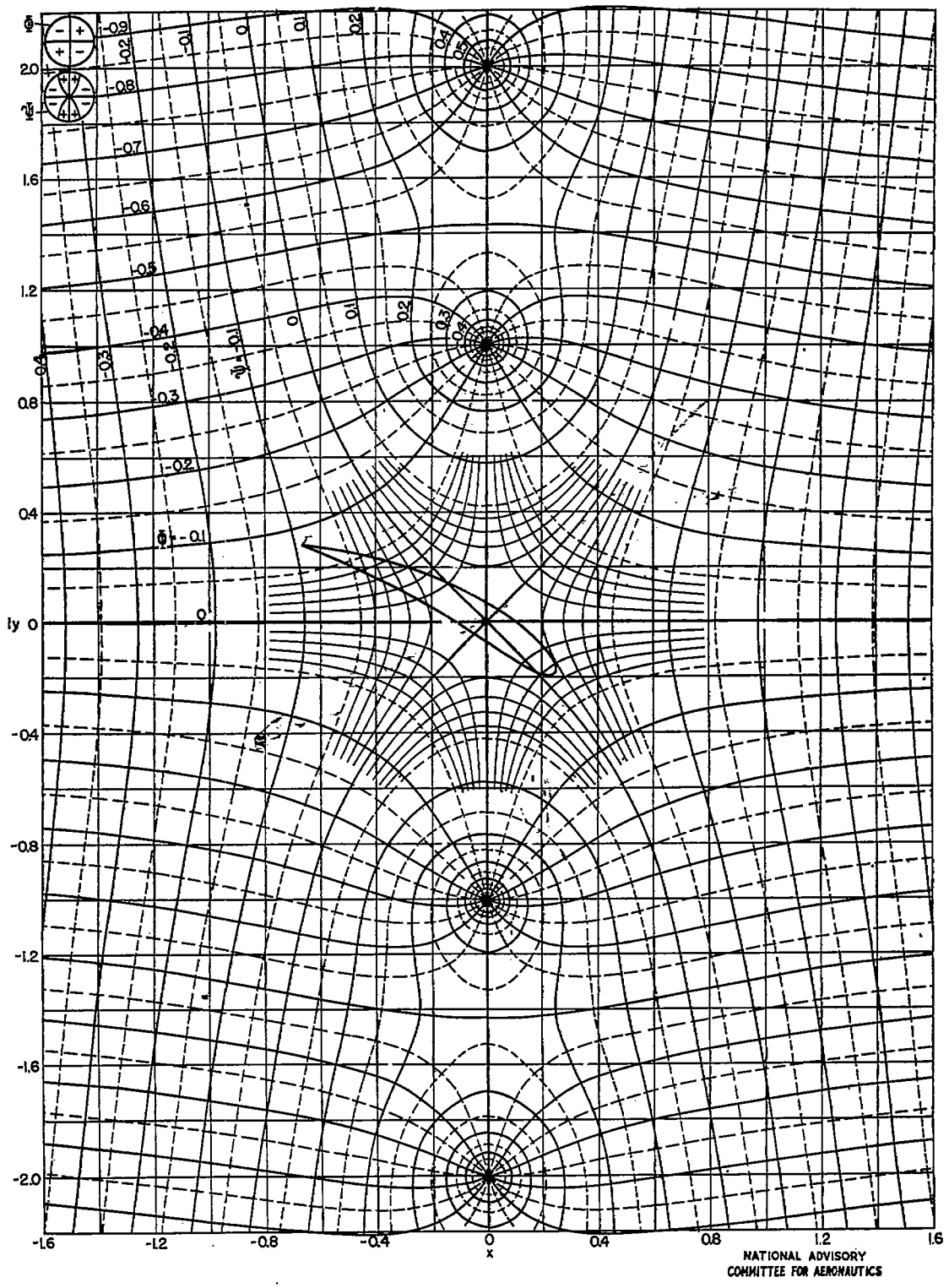

Figure 2.- Velocity potential and stream function for a row of vortices of unit strength spaced at unit distance along the y-axis with the central vortex omitted.

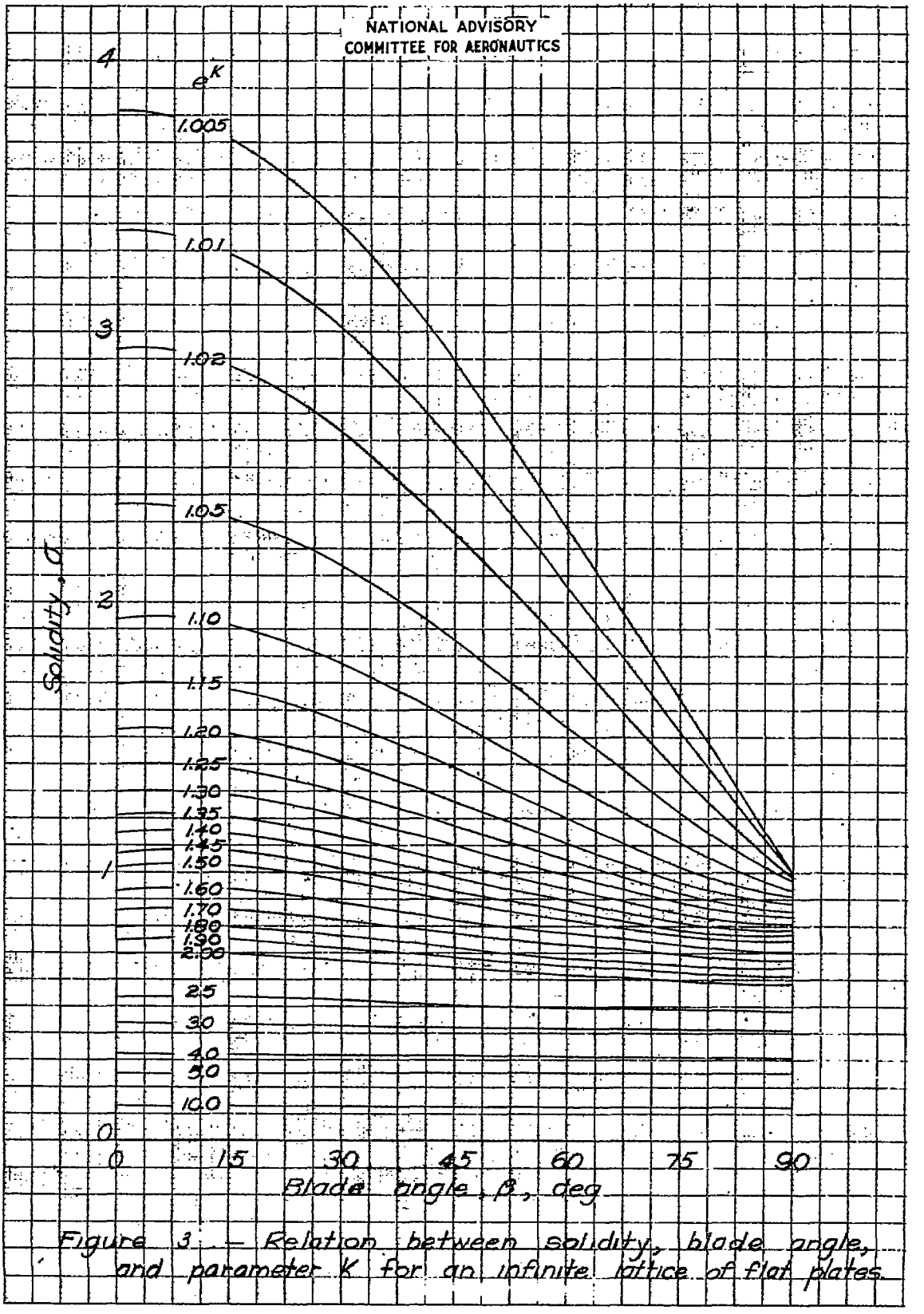

Figure 3. — Relation between solidity, blade angle, and parameter K for an infinite lattice of flat plates.

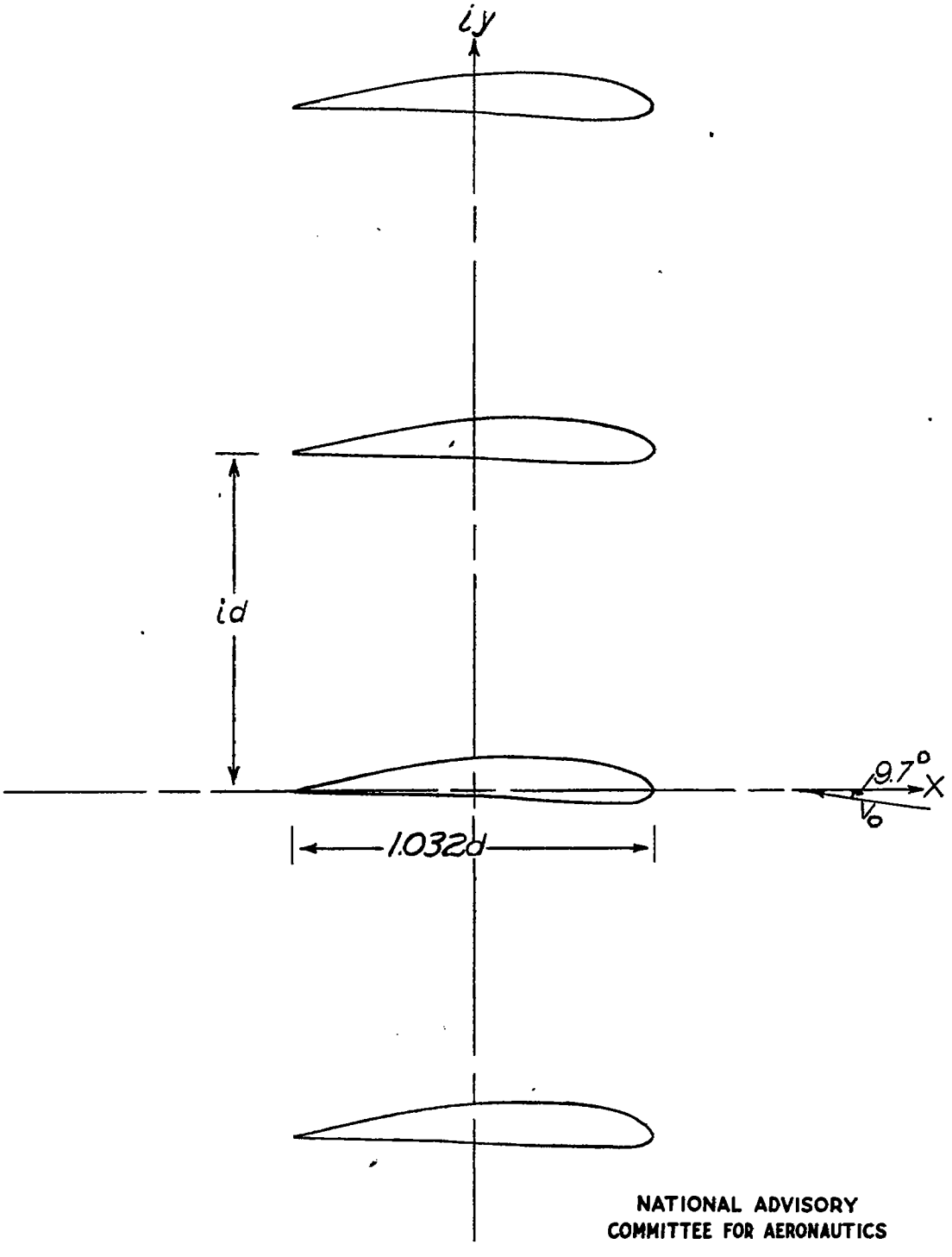

Figure 4.- NACA 4412 airfoil in lattice arrangement. $\beta=0^\circ$; $\sigma=1.032$; $\lambda_0 = 9.7^\circ$.

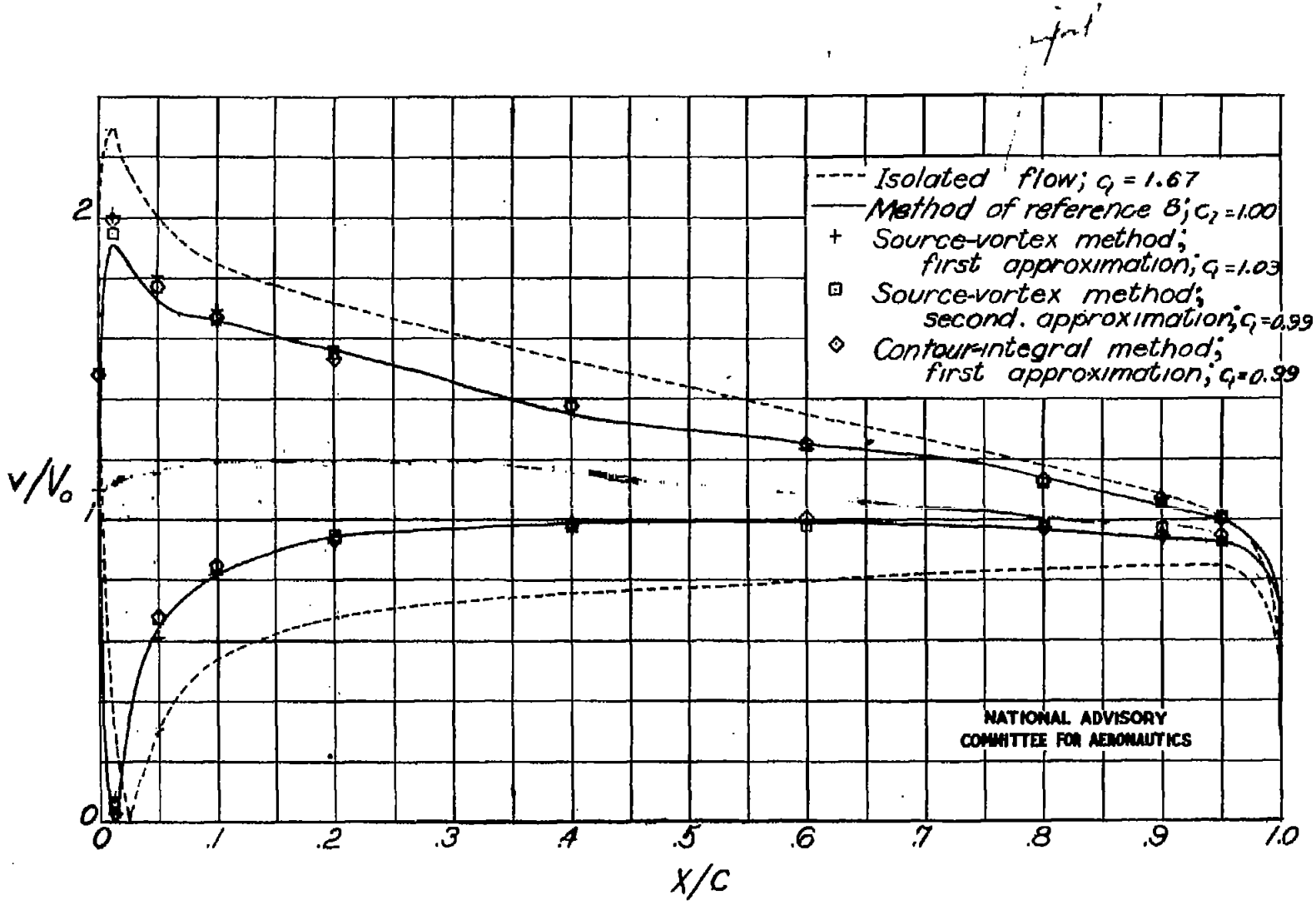

Figure 5 .- Velocities on NACA 4412 airfoil in isolated flow and in lattice arrangement. $\beta = 0^0$; $\sigma = 1.032$; $\alpha_c = 9.7^0$.

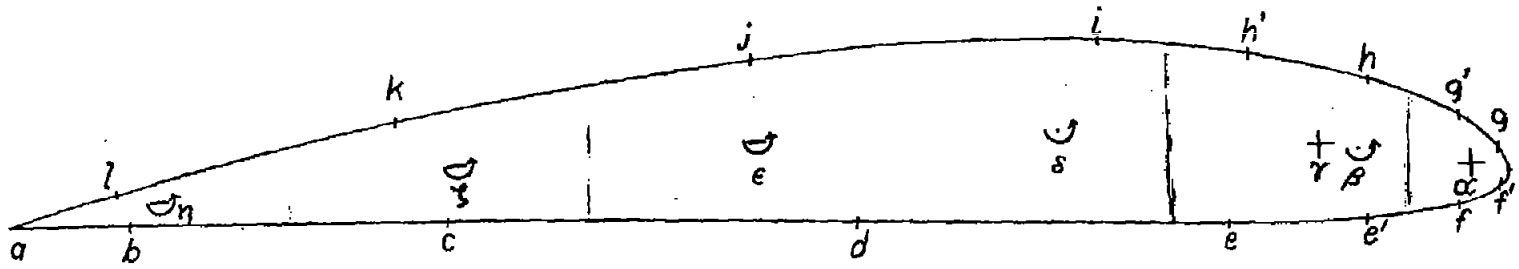

Figure 6.- NACA 4412 airfoil, showing chosen locations of sources and vortices along mean line, and locations at which chart readings were taken.

.08 X .115 = .97
.12 X 1.1 = .132

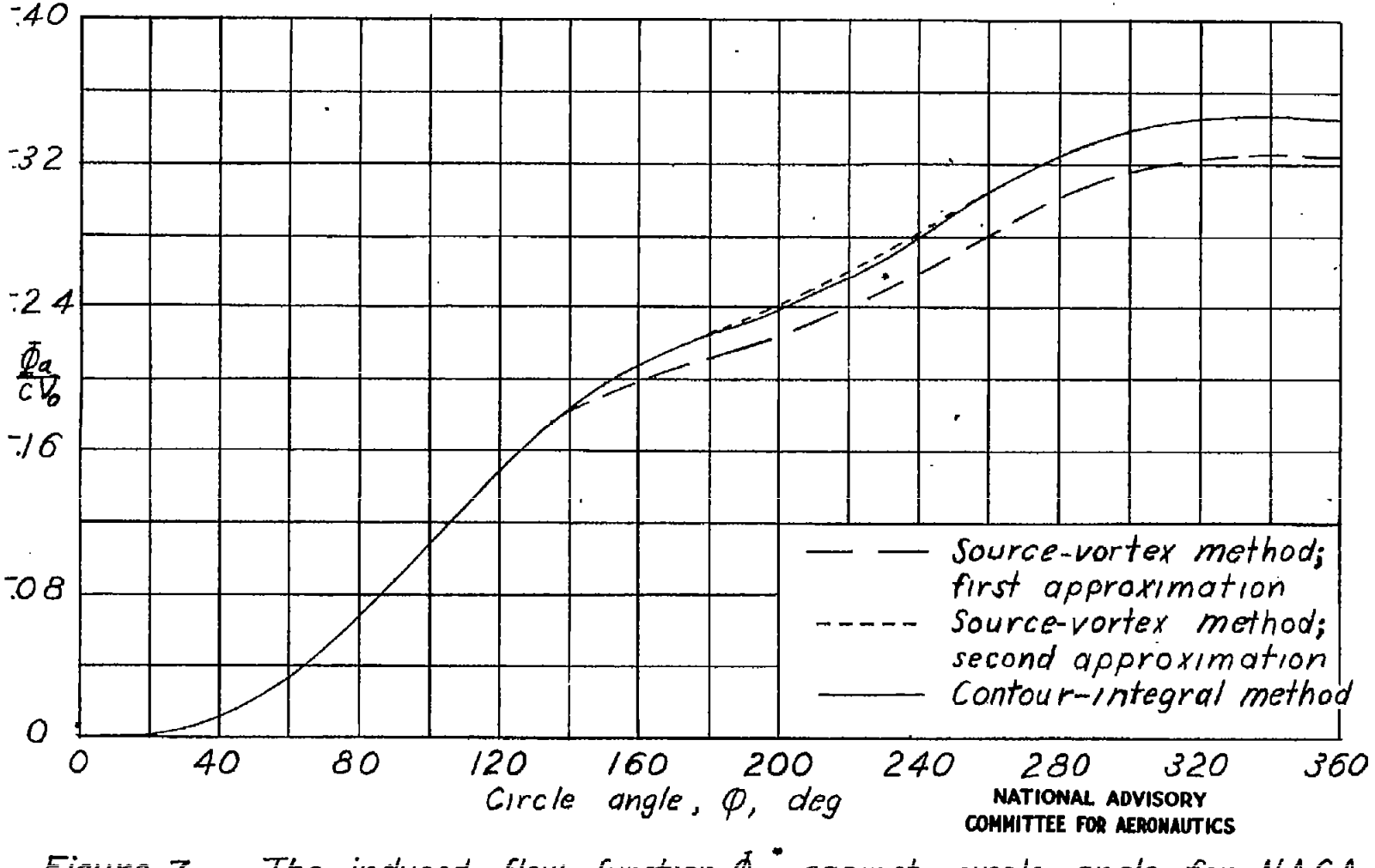

Figure 7 .— The induced flow function Φ_a^* against circle angle for NACA 4412 airfoil in lattice arrangement. $\beta = 0^\circ$; $\sigma = 1.032$; $\alpha_0 = 9.7^\circ$.

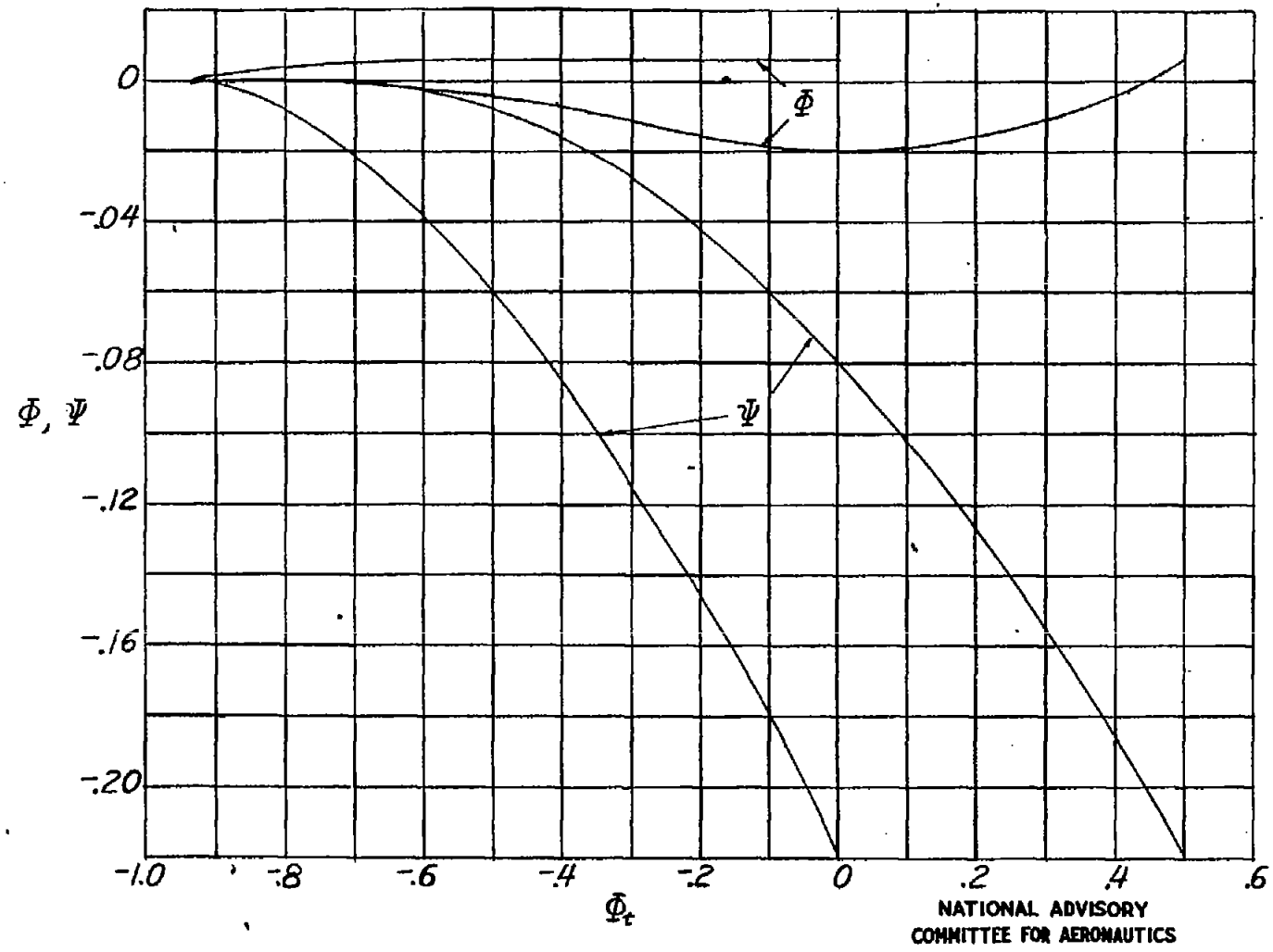

Figure 8.- Typical curves for determination of Φ_d and Ψ_d by contour-integral method. These curves are for point g on NACA 4412 airfoil in lattice arrangement. $\beta = 0^\circ$; $\sigma = 1.032$; $\alpha_0 = 9.7^\circ$.

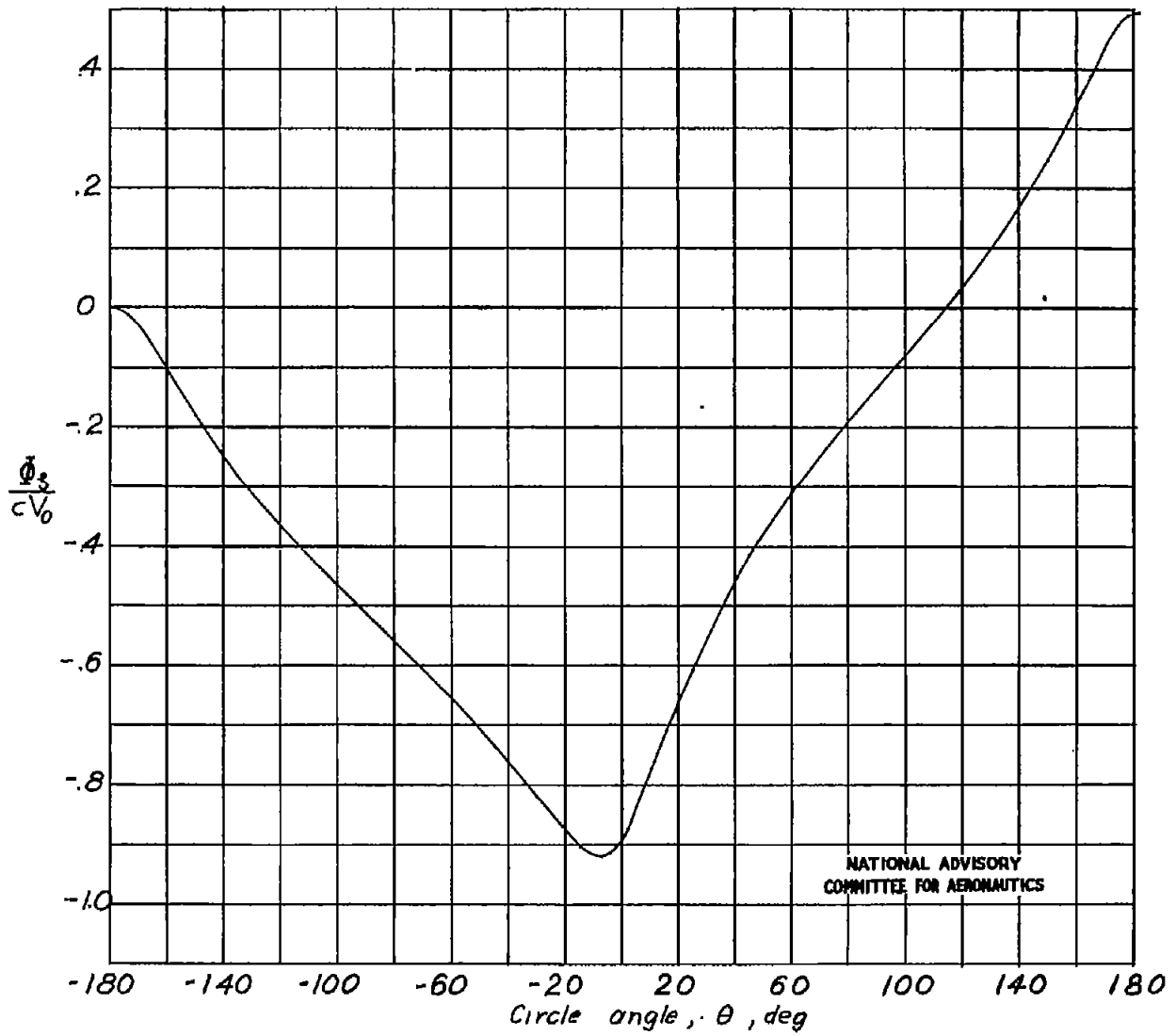

Figure 9 .– Velocity potential on unit circle in ζ-plane, for NACA 4412 airfoil in lattice arrangement. $\beta = 0°$; $\sigma = 1.032$; $\alpha_0 = 9.7°$.

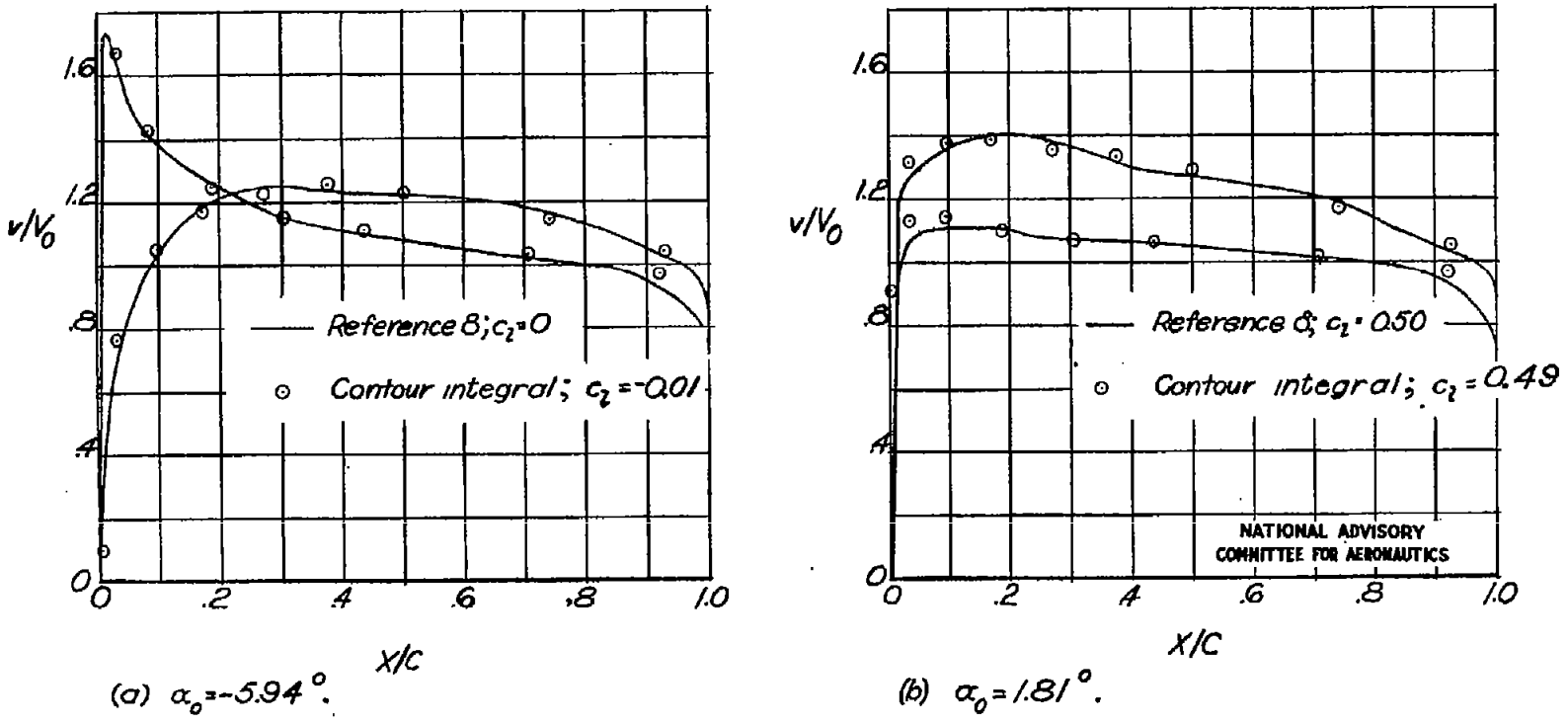

Figure 10. - Velocity distributions on NACA 4412 airfoil in lattice arrangement. $\sigma = 1.032$; $\beta = 0°$.

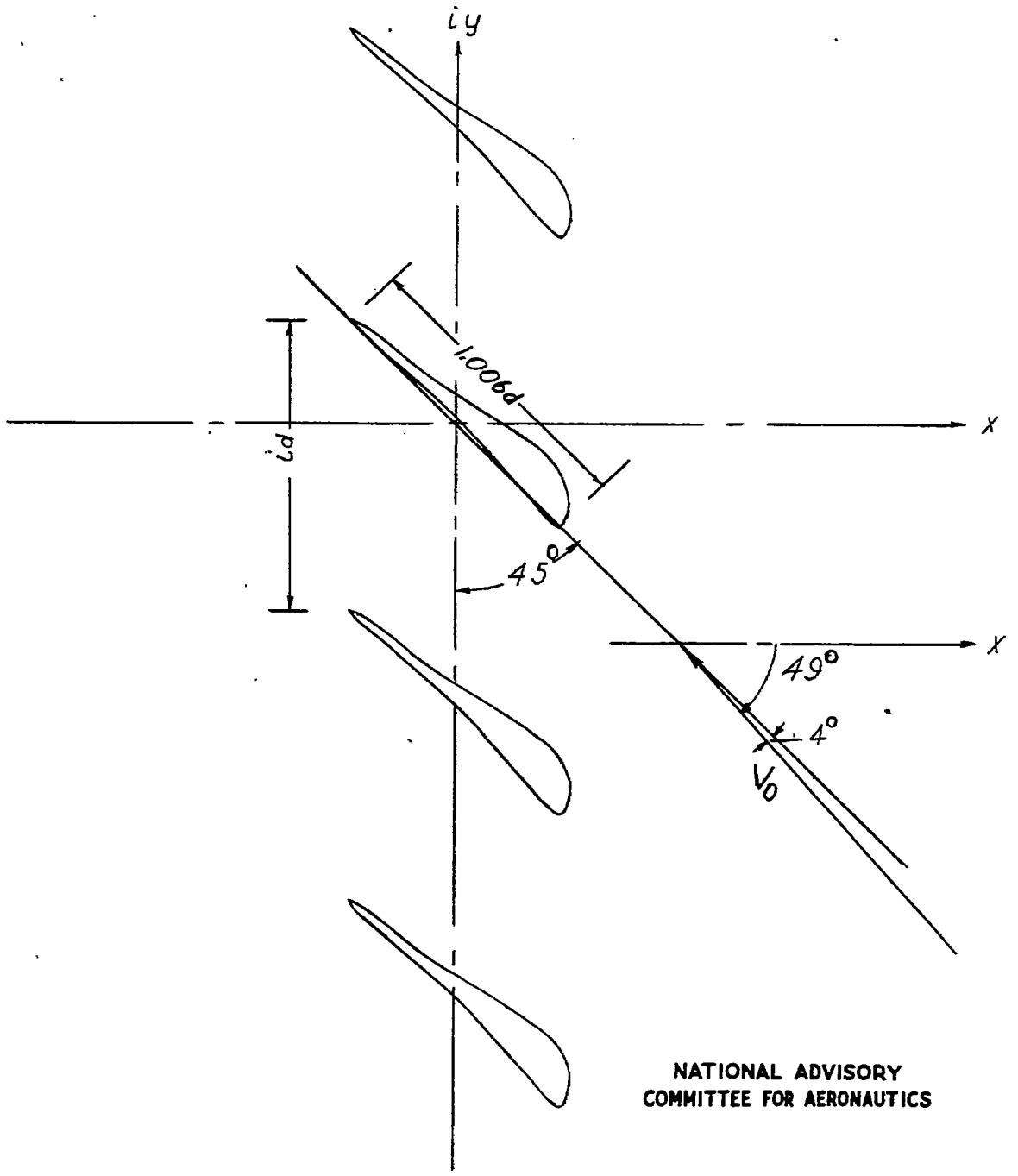

Figure 11 .—Derived airfoil lattice. $\beta = 45°$; $\sigma = 1.006$; $\lambda_0 = 49°$.

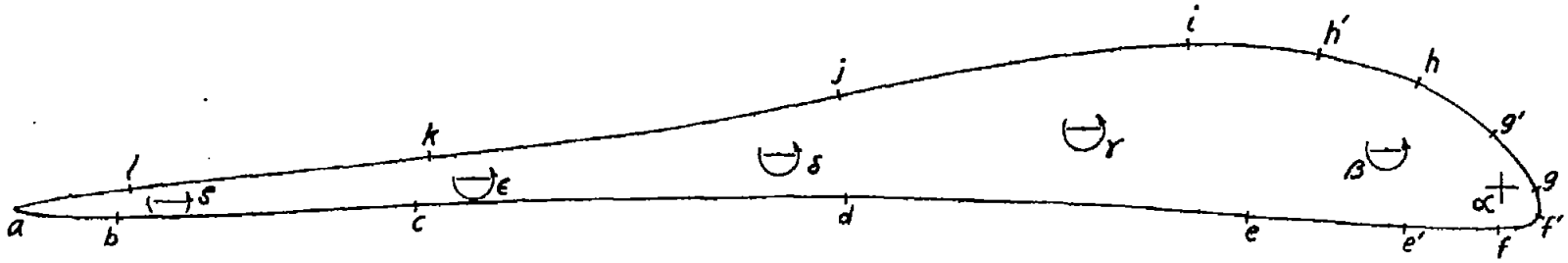

NATIONAL ADVISORY
COMMITTEE FOR AERONAUTICS

Figure 12.- Derived airfoil showing chosen locations of sources and vortices along mean line and locations at which chart readings were taken.

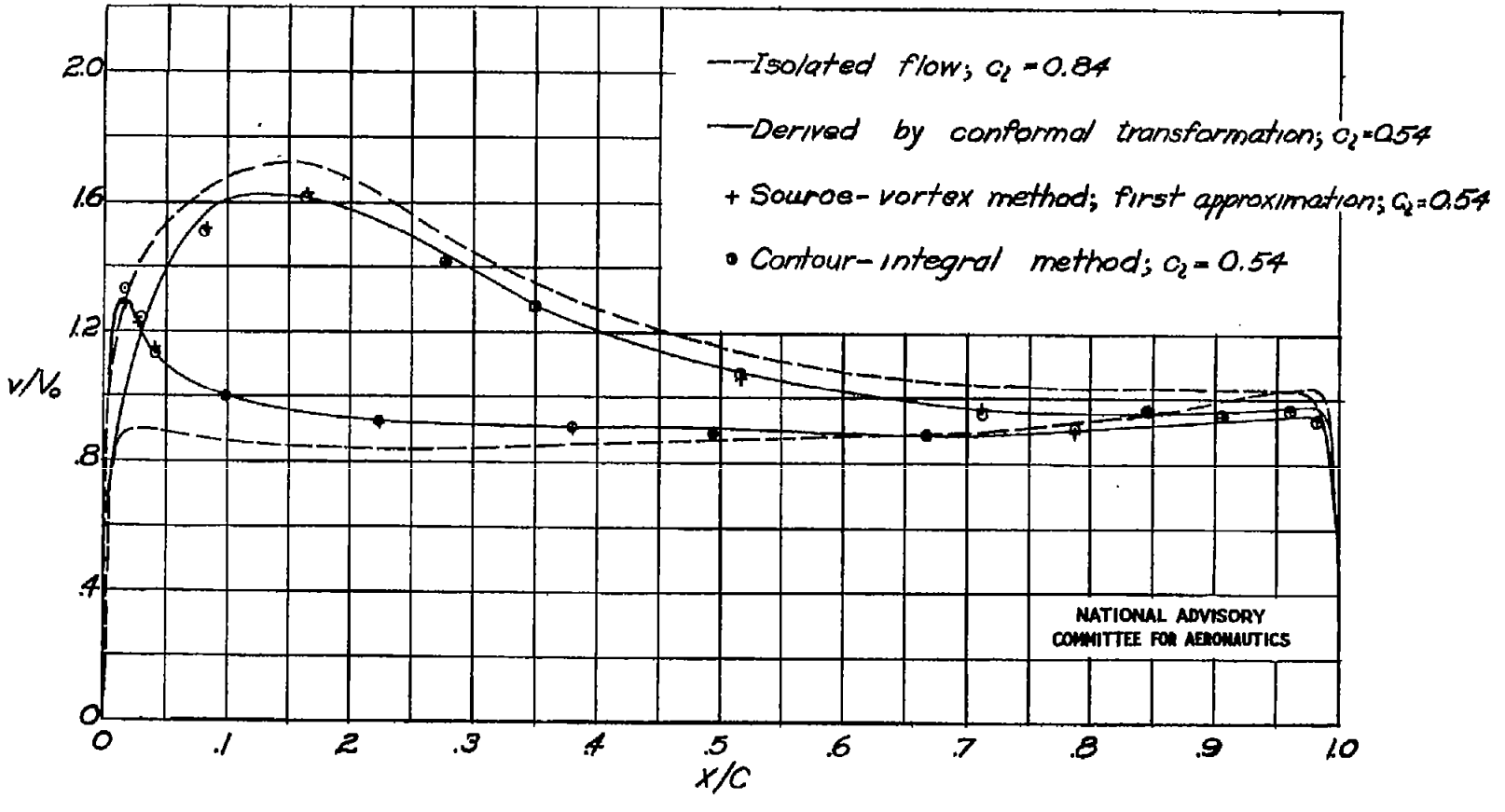

Figure 13 .- Velocities on derived airfoil lattice. $\beta = 45°$; $\sigma = 1.006$; $\lambda_0 = 49°$.

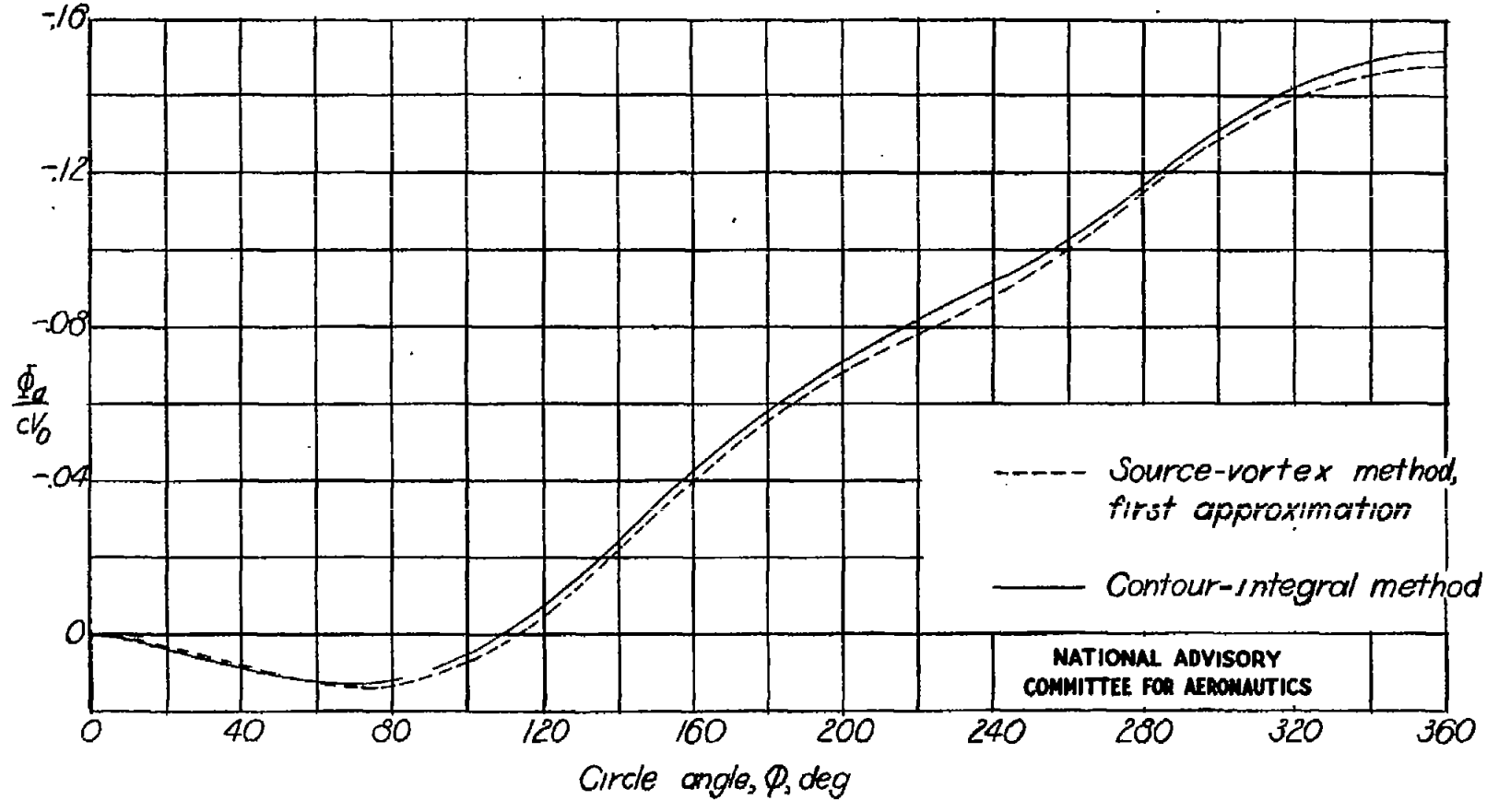

Figure 14. - The induced flow function Φ_a against circle angle for the derived airfoil lattice, $\beta = 45°$; $\sigma = 1.006$; $\lambda_0 = 49°$.

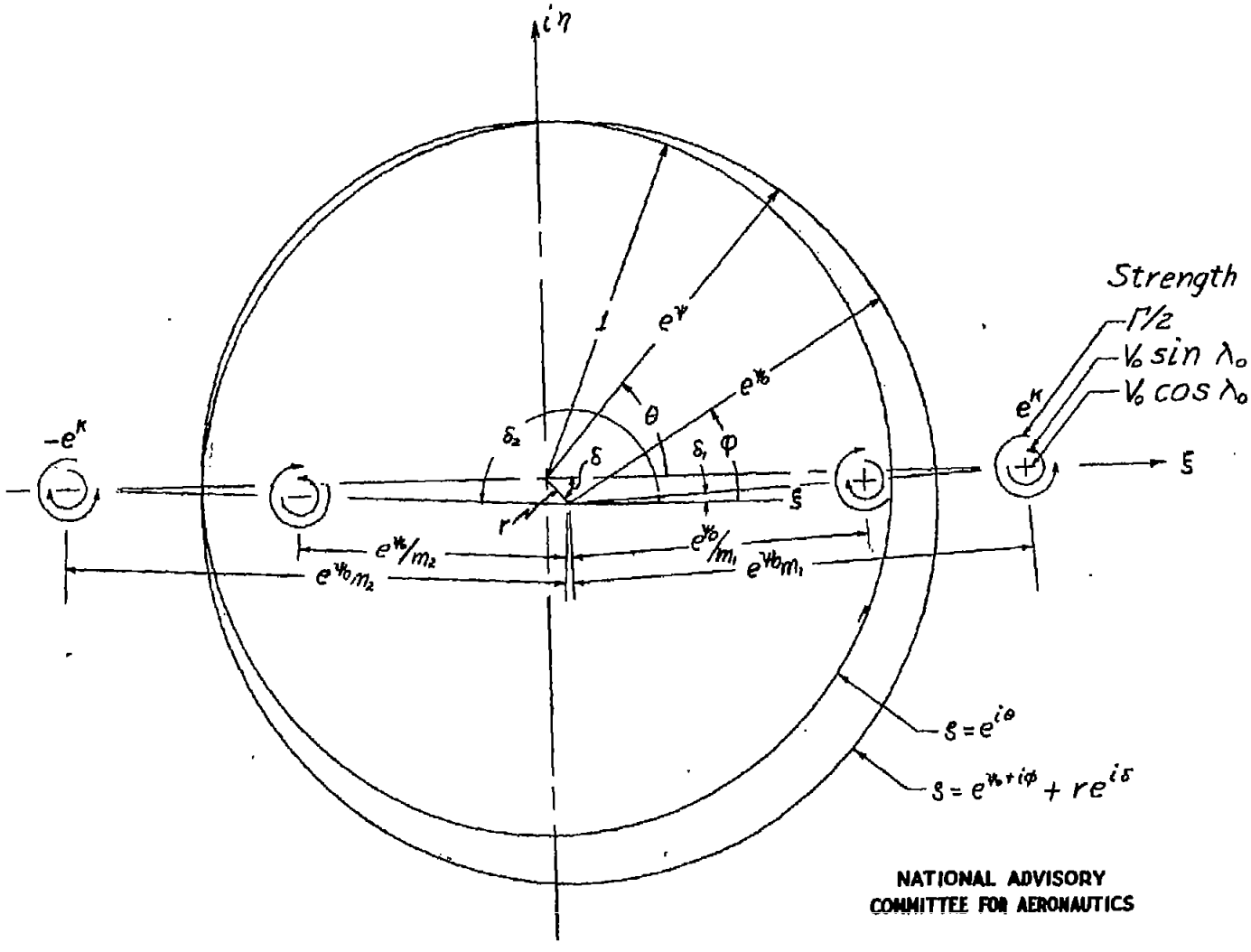

Figure 15 .- Flow singularities in s-plane for derived airfoil lattice.